NASA Technical Memorandum 85776

Low-Speed Wind-Tunnel Study of the High-Angle-of-Attack Stability and Control Characteristics of a Cranked-Arrow-Wing Fighter Configuration

Sue B. Grafton

MAY 1984

NASA

NASA Technical Memorandum 85776

Low-Speed Wind-Tunnel Study of the High-Angle-of-Attack Stability and Control Characteristics of a Cranked-Arrow-Wing Fighter Configuration

Sue B. Grafton
Langley Research Center
Hampton, Virginia

National Aeronautics
and Space Administration

**Scientific and Technical
Information Branch**

1984

SUMMARY

An investigation was conducted in the Langley 30- by 60-Foot Tunnel to study the low-speed, high-angle-of-attack stability and control characteristics of a fighter configuration incorporating a cranked arrow wing. The study was conducted as part of a NASA/General Dynamics cooperative research program to investigate the application of advanced wing designs to combat aircraft. Tests were conducted on a baseline configuration and on several modified configurations. The modifications included a wing apex notch, a wing trailing-edge extension, and wing fences. The results of the investigation showed that the baseline configuration exhibited a high level of maximum lift but displayed undesirable longitudinal and lateral-directional stability characteristics at high angles of attack. Various modifications were made which improved the longitudinal and lateral-directional stability characteristics of the configuration at high angles of attack. However, most of the modifications were detrimental to maximum lift.

INTRODUCTION

A cooperative research program between the NASA Langley Research Center and General Dynamics to investigate the application of advanced wing designs to combat aircraft was recently completed (ref. 1). From the results of this effort, General Dynamics is developing an advanced F-16 derivative, the F-16XL, which incorporates a highly swept cranked arrow wing. As part of this cooperative program, exploratory low-speed, high-angle-of-attack static stability and control tests were conducted in the Langley 30- by 60-Foot Tunnel on a cranked-arrow-wing fighter configuration to identify problem areas and define modifications for improved stability and control characteristics. Many of the modifications investigated in the subject study were first developed in the 1960's for use on supersonic transport designs (ref. 2).

Some of the basic low-speed stability problems of highly swept arrow wings include (1) pitch-up characteristics at moderate to high angles of attack brought on by vortex breakdown over the wing (refs. 2 and 3) and (2) lateral-directional instability near maximum lift caused by asymmetric vortex breakdown under sideslip. Modifications to the basic wing which are aimed at eliminating or minimizing these problems generally destroy vortex lift and significantly reduce the low-speed maximum lift coefficient of the wing (refs. 4, 5, and 6). Also, such modifications can have a detrimental impact on supersonic aerodynamic performance and would be unacceptable. Thus, the challenge in low-speed, high-angle-of-attack research is to provide alterations to the basic arrow-wing design to give acceptable low-speed stability and control characteristics by using several options, which have to be evaluated supersonically.

The present investigation was conducted using a 0.15-scale modified F-16A model to represent an early F-16XL configuration. The model used the fuselage and horizontal tail of the F-16A and incorporated a highly swept cranked-arrow-wing design (ref. 1). The basic configuration was tested with modified leading and trailing edges and with fences on the upper surface. All the configurations were static force tested over wide ranges of angle of attack and angle of sideslip at a free-stream

velocity of 75 ft/sec, which corresponds to a Reynolds number of 2.15×10^6. A limited number of flow-visualization tests were made to provide information for interpreting the force-test results.

SYMBOLS

Static longitudinal forces and moments are referred to the wind-axis system, and static lateral-directional forces and moments are referred to the body-axis system. All force-test data are referred to a moment reference center located longitudinally at 45 percent of the wing mean aerodynamic chord. All measurements were reduced to standard coefficient form on the basis of the geometric characteristics of the wing.

b	wing span, ft
$\bar{c}$	mean aerodynamic chord, ft
C_D	drag coefficient, $F_D/q_\infty S$
C_L	lift coefficient, $F_L/q_\infty S$
C_l	rolling-moment coefficient, $M_X/q_\infty Sb$
C_m	pitching-moment coefficient, $M_Y/q_\infty S\bar{c}$
C_n	yawing-moment coefficient, $M_Z/q_\infty Sb$
C_Y	side-force coefficient, $F_Y/q_\infty S$
F_D	drag force, lb
F_L	lift force, lb
F_Y	side force, lb
I_X	moment of inertia about X body axis, slug-ft^2
I_Z	moment of inertia about Z body axis, slug-ft^2
M_X	rolling moment, ft-lb
M_Y	pitching moment, ft-lb
M_Z	yawing moment, ft-lb
q_∞	free-stream dynamic pressure, lb/ft^2
S	wing area, ft^2
X,Y,Z	body reference axes
α	angle of attack, deg
β	angle of sideslip, deg

Derivatives:

$$C_{l_\beta} = \frac{\partial C_l}{\partial \beta} \qquad C_{n_\beta} = \frac{\partial C_n}{\partial \beta} \qquad C_{Y_\beta} = \frac{\partial C_Y}{\partial \beta}$$

$$C_{n_{\beta,dyn}} = C_{n_\beta} \cos \alpha - \frac{I_Z}{I_X} C_{l_\beta} \sin \alpha$$

MODEL

The wind-tunnel model consisted of a 0.15-scale modified F-16A fuselage, which has a flow through duct, and a cranked-arrow-wing planform. A three-view sketch of the basic configuration is presented in figure 1. The geometric characteristics of the test model are listed in table I. Sketches showing a wing leading-edge apex modification, a wing trailing-edge modification, and a wing fence modification are shown in figure 2. The force-test model, constructed primarily of molded fiberglass and wood, was a 0.15-scale model of the proposed full-scale airplane. The wings were constructed without control surfaces.

TUNNEL AND APPARATUS

The tests were conducted in the Langley 30- by 60-Foot Tunnel. The model support system used in the force tests is shown in figure 3. As reported in reference 3, certain model support systems can cause large flow interference problems when used to test configurations which produce strong vortex flows at high angles of attack. The model support system shown in figure 3 was designed to minimize these interference problems. The data were measured at a free-stream velocity of 75 ft/sec, which corresponds to a Reynolds number of 2.15×10^6 based on the mean aerodynamic chord of the wing. The force-test setup used a strut-mounted system and incorporated a six-component internally mounted strain-gage balance. The model engine inlet and exit were open for all tests.

TESTS

Static-force tests were conducted over an angle-of-attack range from -4° to 41° at sideslip angles from -13.5° to 10.5°. Tests were also conducted to study the effects of the wing leading- and trailing-edge modifications and wing fences described earlier.

In addition to the static tests, a limited number of smoke flow tests were made to help identify flow behavior over the wing. The smoke flow tests were used to document vortex flow behavior and to establish a relationship between vortex flow breakdown as a function of angle of attack and angle of sideslip for use in interpreting the static-force test data.

RESULTS AND DISCUSSION

Baseline Configuration

Longitudinal aerodynamic characteristics.- The longitudinal characteristics of the baseline configuration with and without the vertical tail are presented in figure 4. The data show that the configuration exhibited a high level of lift, achieved maximum lift near an angle of attack of 36°, and exhibited a high level of longitudinal instability or pitch-up at angles of attack above about 10°. As expected, the data show that removing the vertical tail had relatively little effect on the longitudinal aerodynamic characteristics. The severe pitch-up tendency is characteristic of highly swept wings at low speeds and is well documented in earlier publications (for example, refs. 2 and 3). The pitch-up instability is mainly associated with the formation of highly concentrated vortex flow emanating from the wing apex at moderate to high angles of attack. The vortex core tends to lift off the surface of the aft portion of the wing while remaining close to the surface of the forward portion. The loss in vortex-induced lift over the aft portion of the wing tends to shift the aerodynamic center forward to produce the pitch instability. At the higher angles of attack, the problem is further aggravated by vortex breakdown, which starts at the rear of the wing and moves forward with increasing angle of attack. Figure 5 presents photographs of smoke flow studies on the baseline configuration at high angles of attack. The photographs show that vortex breakdown started at the wing trailing edge near $\alpha = 25°$ and progressed forward with increasing angle of attack until it reached the wing apex near $\alpha = 35°$. The photographs also show that sideslipping the model increased the angle of attack for vortex breakdown on the leeward wing and reduced the angle of attack for vortex breakdown on the windward wing.

Lateral-directional stability characteristics.- The variation of the static lateral-directional force and moment coefficients with angle of sideslip for the baseline configuration is presented for various values of angle of attack in figure 6. The data show that the variations of C_n and C_l with sideslip were fairly linear at angles of attack below 31° and extremely nonlinear at angles of attack of 31° and 36°. The data of figures 7 and 8 show that the vertical tail was ineffective by $\alpha = 31°$ and actually produced highly destabilizing yawing-moment and rolling-moment increments at $\alpha = 41°$. The data of figures 6 and 7 are summarized in figure 8 in terms of the lateral-directional stability derivatives C_{Y_β}, C_{n_β}, and C_{l_β}. The derivatives were obtained from the coefficient data by the slope method using the data points $\beta = 4.5°$ and $\beta = -5.5°$. The results show that the model with the vertical tail removed was directionally unstable throughout the α range with the instability increasing sharply above $\alpha = 30°$. The dihedral effect $\left(-C_{l_\beta}\right)$ was stable up to $\alpha = 30°$ but showed an abrupt destabilizing break near $\alpha = 32°$. The addition of the vertical tail produced directional stability for angles of attack up to about 27°. Above $\alpha = 21°$, the increment in directional stability provided by the vertical tail decreased rapidly, and the model became directionally unstable above $\alpha = 27°$. The destabilizing effect of the vertical tail above $\alpha = 31°$ indicates that the tail was in an adverse sidewash field. The vertical tail increased the stable dihedral effect at low and moderate angles of attack but became laterally destabilizing at higher angles of attack. This destabilizing effect resulted in the baseline configuration exhibiting lateral instability in the angle-of-attack range from 33° to 40°.

The lateral instability at high angles of attack is attributed mainly to the asymmetrical breakdown of the wing leading-edge vortices under sideslip. The effect of sideslip angle on vortex breakdown, shown in the photographs of figure 5, is discussed in more detail in reference 2. Other investigations (see refs. 3 and 4) have documented the predominant effect of the asymmetric vortex breakdown on rolling-moment characteristics at high angles of attack for configurations with highly swept wings. This loss in lateral stability combined with the highly unstable directional-stability characteristics made the configuration highly susceptible to yaw divergence, as shown by the $C_{n_{\beta,dyn}}$ data presented in figure 9. Negative values of $C_{n_{\beta,dyn}}$ indicate susceptibility to directional divergence, as described in reference 5. The baseline configuration is seen to have unstable or negative values of $C_{n_{\beta,dyn}}$ above $\alpha = 32°$. These negative values of $C_{n_{\beta,dyn}}$ are caused by the unstable values of C_{n_β} and neutral or unstable values of C_{l_β}. To correct this lateral-directional stability problem and the severe pitch-up discussed earlier, a number of configuration modifications were studied, and the results are discussed in the subsequent section.

Modified Configurations

Longitudinal aerodynamic characteristics.- In an attempt to alleviate the pitch and lateral-directional instabilities discussed above, the vertical tail was removed from the baseline configuration, and various alterations were made in order to develop a modified configuration. The modifications included a wing apex notch, a wing trailing-edge extension, and wing fences (fig. 2). Because the instabilities were a direct result of the wing leading-edge vortex flow characteristics, each modification was designed to favorably alter these characteristics.

Presented in figure 10 are the results of tests to study the effect of the wing apex notch modification on the longitudinal aerodynamic characteristics of the configuration. This modification, shown in figure 2(a), produced a large stabilizing effect and significantly reduced the instability above $\alpha = 11°$. The modification caused some reduction in lift coefficient above $\alpha = 15°$. This reduction in lift coefficient was apparently a result of the apex notch, which weakened the wing leading-edge vortex.

Another modification made specifically to minimize pitch instability was the wing trailing-edge extension. (See fig. 2(b).) The data of figure 11 show that the trailing-edge extension was effective in reducing the pitch instability and, as expected, increased the maximum lift because of the increased wing area. Presented in figure 12 are data obtained from tests to determine the effectiveness of the combination of apex notch and wing trailing-edge extension on the longitudinal aerodynamic characteristics. The data of figure 12 show that the combined effects of apex notch and wing trailing-edge extension produced a very favorable effect on pitching moment and maximum lift. The maximum unstable pitching-moment coefficient was reduced from about 0.10 to 0.023, and the maximum lift coefficient was increased from 1.55 to 1.65.

Another modification studied was the addition of wing fences. (See fig. 2(c).) This modification was aimed primarily at improving the lateral stability at high

angles of attack by forcing the vortices on the right and left wings to break down more symmetrically and thereby minimize the adverse effect of asymmetrical vortex breakdown on lateral stability. The results of adding the wing fences on longitudinal characteristics are presented in figure 13 and show that wing fences reduced the level of pitch instability above $\alpha = 25°$ but were very detrimental to vortex lift, as indicated by the reduction in the lift-curve slope and loss of maximum lift.

The results of tests to study the combined effects of the wing apex notch, wing trailing-edge extension, and wing fences on the longitudinal aerodynamic characteristics are summarized in figure 14. The data show that the combined modifications greatly reduced the pitch instability, although the configuration still showed a mild pitch-up near $\alpha = 11°$. The modification also reduced the lift coefficient above $\alpha = 16°$. Comparing figure 14 with figure 15 shows that the addition of the vertical tail had little effect on these results.

Lateral-directional stability characteristics.- Presented in figure 16 are the lateral-directional stability characteristics of the baseline configuration compared with those of the modified configuration with the apex notch. The data show some slight detrimental effects of the notch on the directional stability characteristics. However, the notch appeared to provide some improvement in lateral stability near $\alpha = 36°$. The effect of the wing trailing-edge extension on the lateral-directional stability characteristics is shown in the data of figure 17. The data show very little effect of trailing-edge extension on the directional stability characteristics but a detrimental effect on lateral stability above $\alpha = 31°$. In fact, the beneficial effect of the apex notch at $\alpha = 36°$ was offset by the detrimental effect of the trailing-edge extension. It should be remembered, however, that the apex notch and trailing-edge extension modifications were aimed primarily at reducing the pitch-up characteristics of the model and that their influence on lateral-directional stability characteristics was of secondary interest. As shown in figure 18, the lateral-directional stability characteristics of the configuration with the combination of the apex notch and trailing-edge extension were somewhat inferior to those of the baseline configuration.

Presented in figure 19 are the results of tests to determine the incremental effect on lateral-directional stability of adding the wing fences. As noted in the earlier discussion of the longitudinal characteristics, the fences were conceived as devices for deliberately forcing vortex breakdown in a more symmetrical fashion, particularly under sideslip conditions, and for alleviating the lateral instability exhibited by the baseline configuration in the region of maximum lift. Although they were detrimental to vortex lift, the fences accomplished their primary purpose and eliminated the lateral instability near $\alpha = 36°$. Figure 20 compares the lateral-directional stability characteristics of the baseline configuration with those of the configuration incorporating all three modifications. The data show that the combination of modifications was generally detrimental to directional stability throughout the angle-of-attack range and reduced the lateral stability below $\alpha = 33°$ while improving it at higher angles of attack.

Presented in figure 21 are the lateral-directional stability characteristics of the baseline and modified configurations with the vertical tail on. The combination of modifications reduced the directional stability at low angles of attack and resulted in the model becoming directionally unstable near $\alpha = 24°$. Above $\alpha = 31°$, the modifications improved directional stability compared with the baseline configuration. The modifications were unfavorable to lateral stability below $\alpha = 31°$ but produced favorable effects at higher angles of attack. The overall impact of the

modifications at high angles of attack can be summarized by using the $C_{n_{\beta,dyn}}$ parameter. The $C_{n_{\beta,dyn}}$ data for the baseline and modified configurations are presented in figure 22. The data show that the modifications reduced the magnitude of $C_{n_{\beta,dyn}}$ at moderate angles of attack; however, the modifications extended the angle-of-attack range for stable values of $C_{n_{\beta,dyn}}$ up to 36°.

CONCLUDING REMARKS

The results of a low-speed, exploratory wind-tunnel study of a cranked-arrow-wing fighter configuration can be summarized as follows:

1. The baseline configuration exhibited a high level of maximum lift but displayed unstable longitudinal and lateral-directional stability characteristics at moderate to high angles of attack. These characteristics were dominated by the strong vortex flows generated by the highly swept wing at these conditions.

2. The combination of wing apex notch, wing trailing-edge extension, and wing fences improved the longitudinal and lateral-directional stability characteristics of the baseline configuration at high angles of attack but were detrimental to maximum lift coefficient.

Langley Research Center
National Aeronautics and Space Administration
Hampton, VA 23665
April 20, 1984

REFERENCES

1. Miller, David S.; and Schemensky, Roy T.: Design Study Results of a Supersonic Cruise Fighter Wing. AIAA Paper 79-0062, Jan. 1979.

2. Freeman, Delma C., Jr.: Low Subsonic Flight and Force Investigation of a Supersonic Transport Model With a Highly Swept Arrow Wing. NASA TN D-3887, 1967.

3. Johnson, Joseph L., Jr.; Grafton, Sue B.; and Yip, Long P.: Exploratory Investigation of the Effects of Vortex Bursting on the High Angle-of-Attack Lateral-Directional Stability Characteristics of Highly-Swept Wings. A Collection of Technical Papers - AIAA 11th Aerodynamic Testing Conference, Mar. 1980, pp. 282-297. (Available as AIAA-80-0463.)

4. Hummel, Dietrich (MacAdam, E. J., transl.): Research on Vortex Breakdown on Slender Delta Wings. A.R.A. Lib. Transl. No. 12, Aircraft Res. Assoc. Ltd., Oct. 1965.

5. Fennell, L. J.: Vortex Breakdown - Some Observations in Flight on the HP 115 Aircraft. R. & M. No. 3805, British A.R.C., 1977.

6. Chambers, Joseph R.; and Anglin, Ernie L.: Analysis of Lateral-Directional Stability Characteristics of a Twin-Jet Fighter Airplane at High Angles of Attack. NASA TN D-5361, 1969.

TABLE I.- GEOMETRIC CHARACTERISTICS OF BASELINE MODEL

Fuselage:	
Length, ft	7.34
Wing:	
Area, ft^2	13.5
Span, ft	4.86
Aspect ratio	1.75
Taper ratio	0.10
Leading-edge sweep:	
Inboard, deg	70
Outboard, deg	50
Trailing-edge sweep, deg	18.5
Dihedral, deg	0
Incidence, deg	0
Mean aerodynamic chord, ft	3.71
Twist, deg	0
Airfoil	NACA 64A003.2
Root chord, ft	6.93
Tip chord, ft	0.58
Vertical tail:	
Area, ft^2	0.55
Span, ft	0.85
Aspect ratio	1.30
Taper ratio	0.30
Leading-edge sweep, deg	37
Trailing-edge sweep, deg	0
Airfoil:	
Root	6 percent biconvex
Tip	3.5 percent biconvex

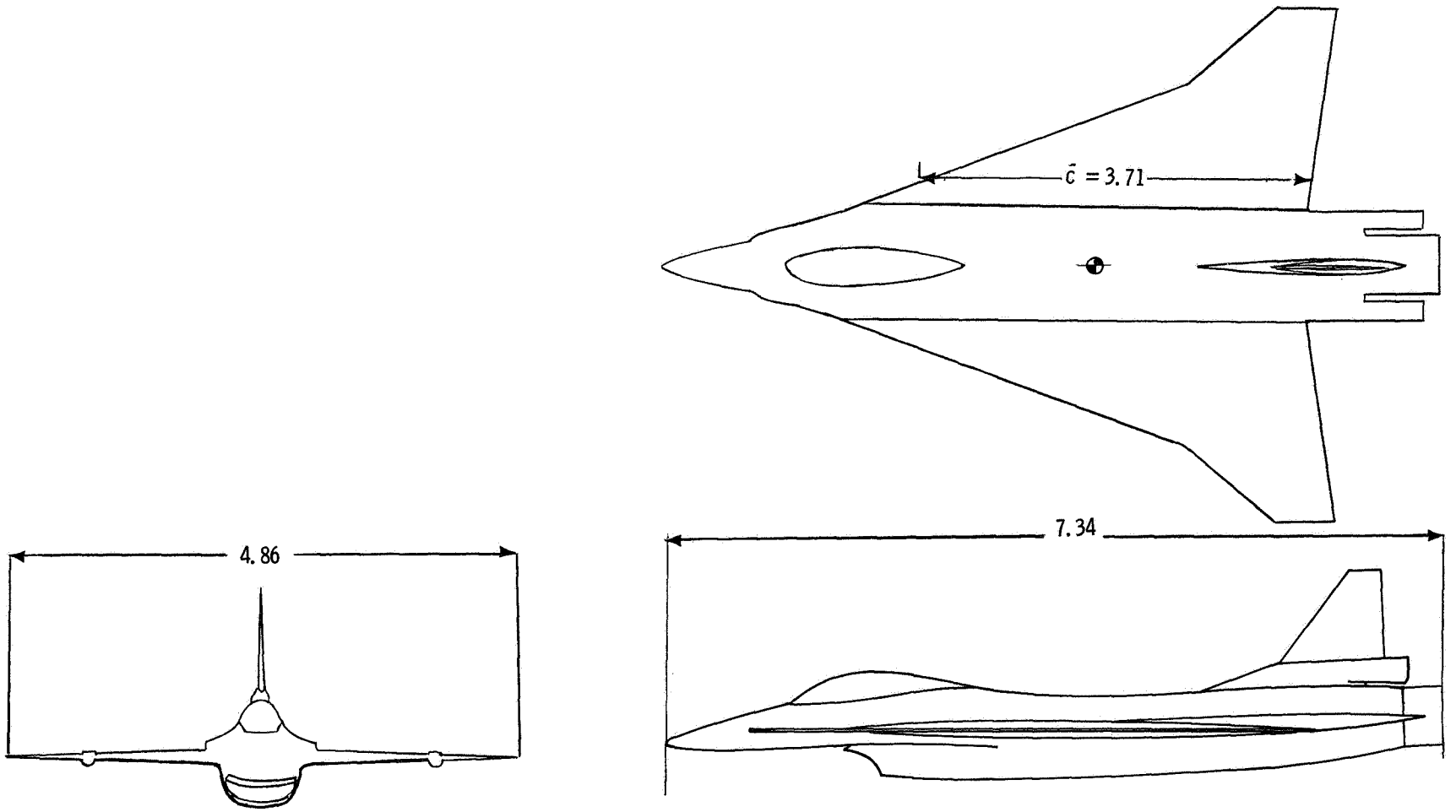

Figure 1.- Three-view sketch of baseline model. Dimensions are given in feet.

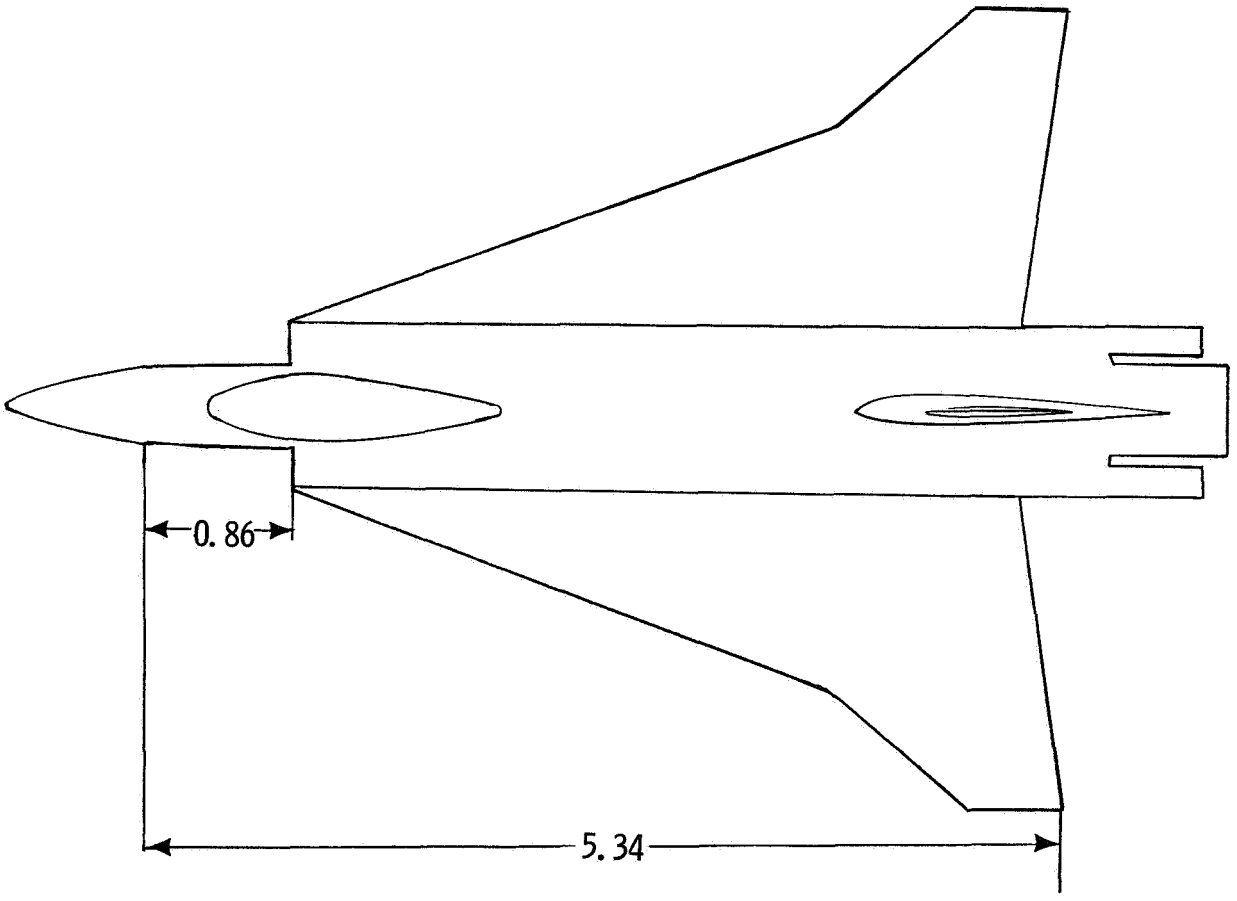

(a) Wing leading-edge apex notch.

Figure 2.- Modifications to baseline configuration. Dimensions are given in feet.

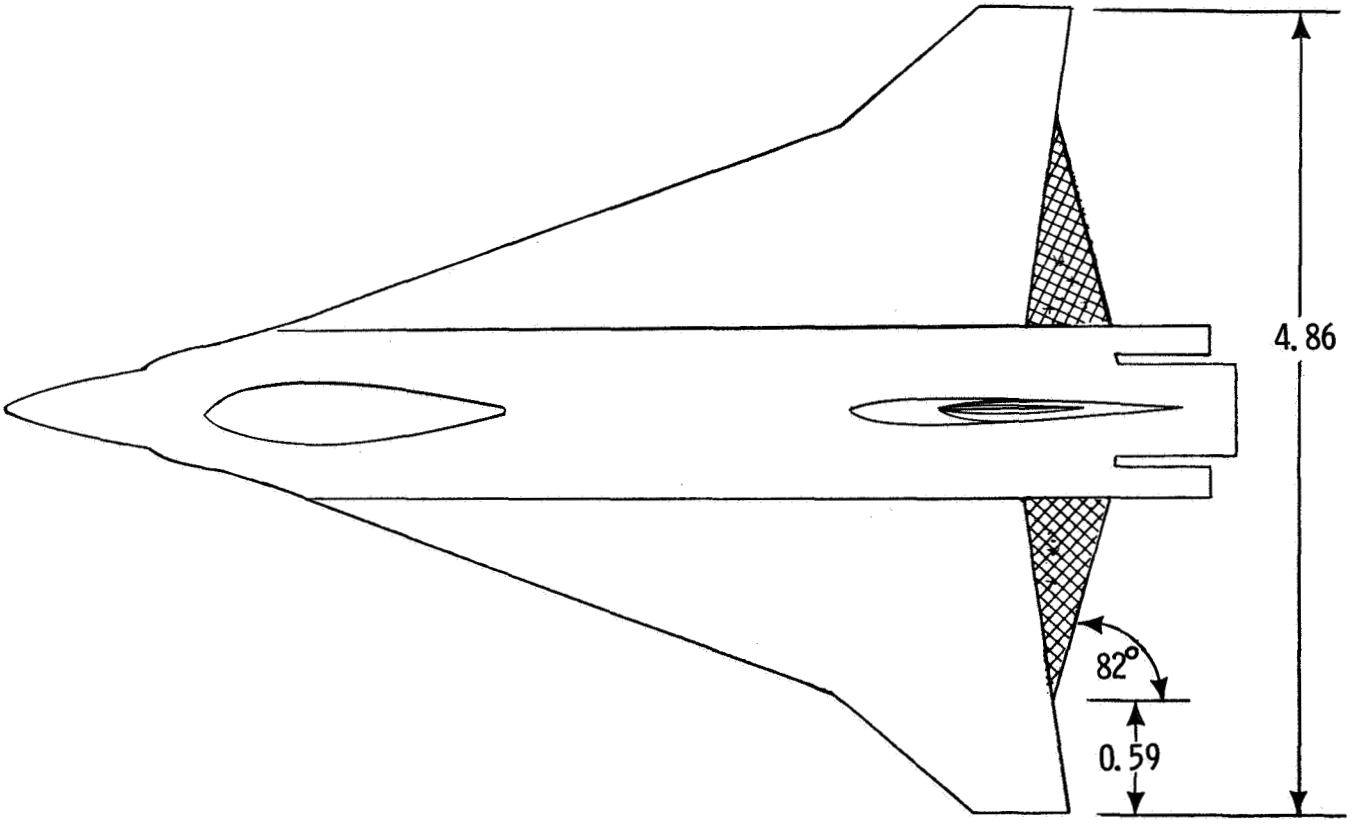

(b) Wing trailing-edge extension.

Figure 2.- Continued.

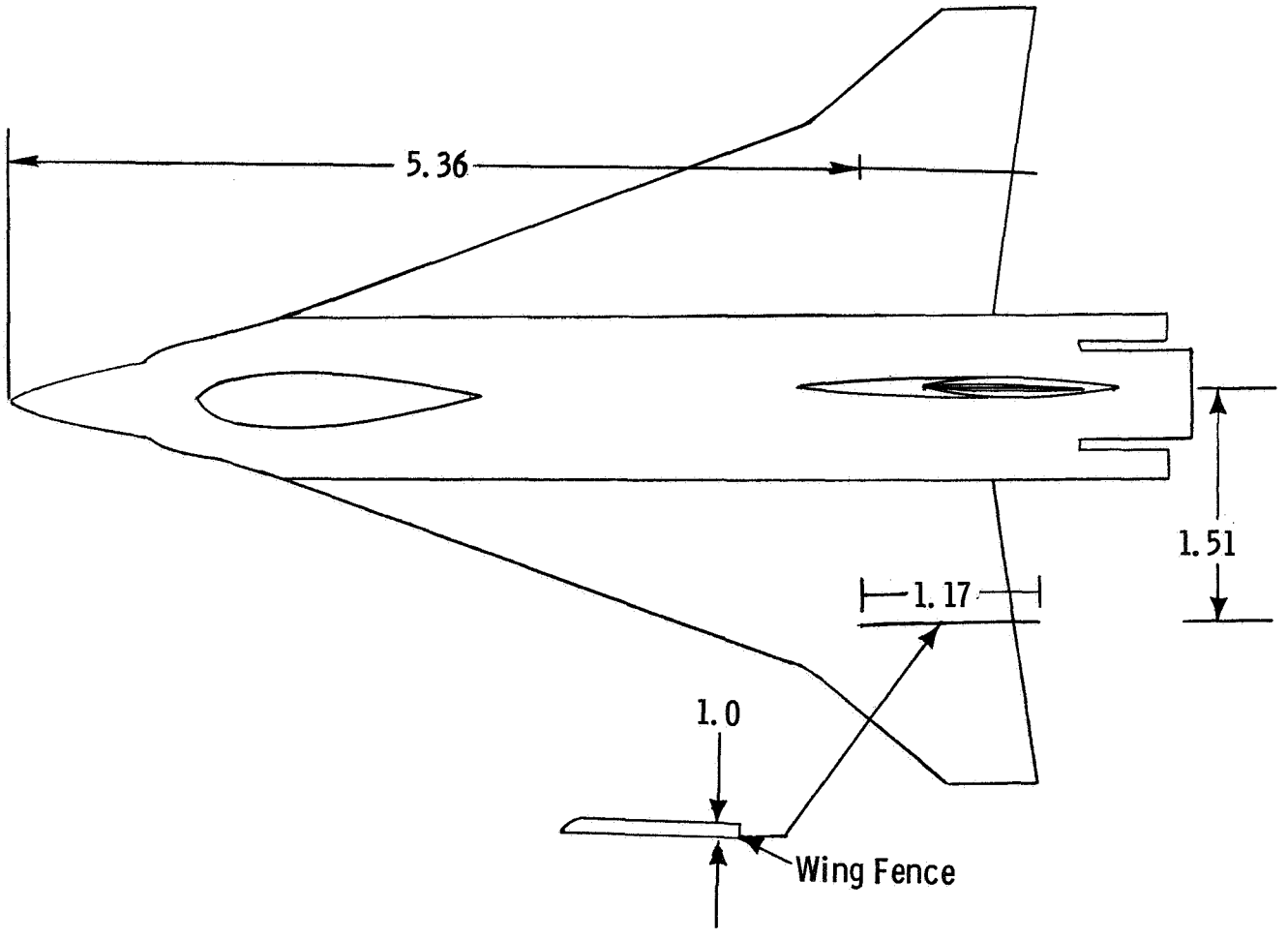

(c) Wing fences.

Figure 2.- Concluded.

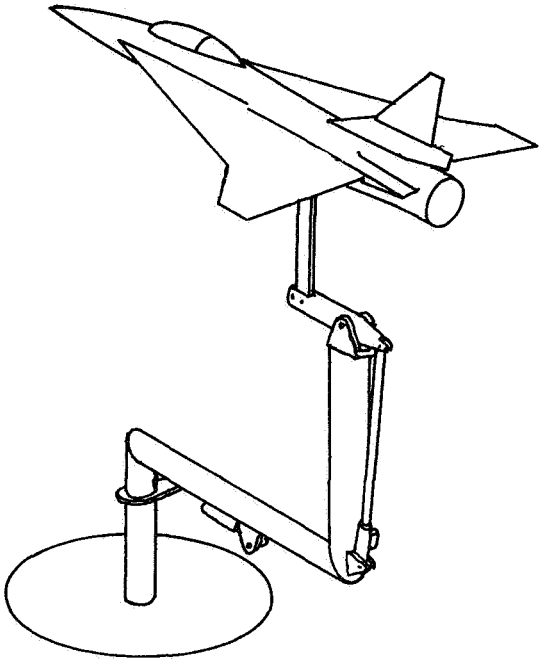

Figure 3.- Model support system
for static-force test.

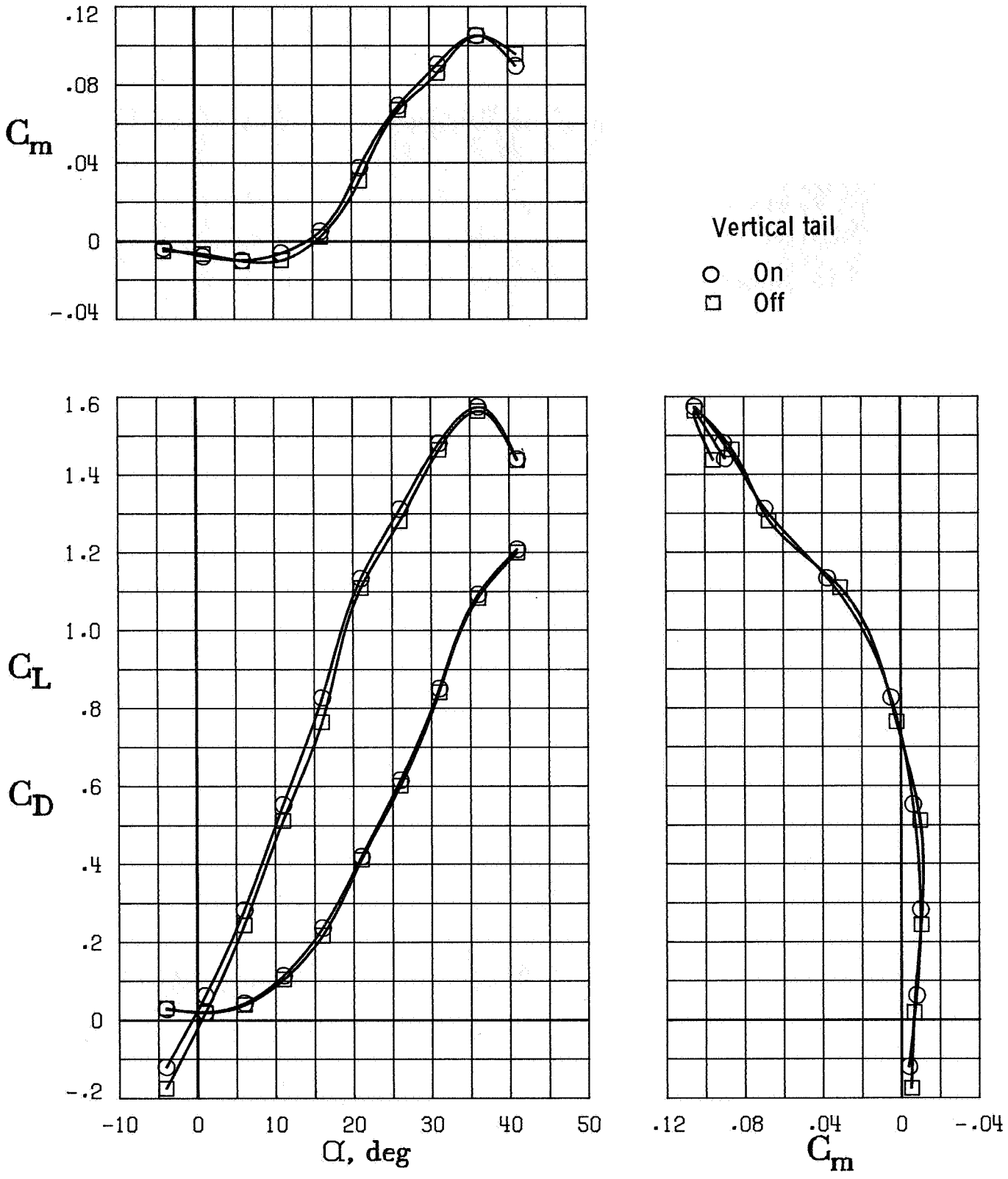

Figure 4.- Static longitudinal aerodynamic characteristics of baseline configuration.

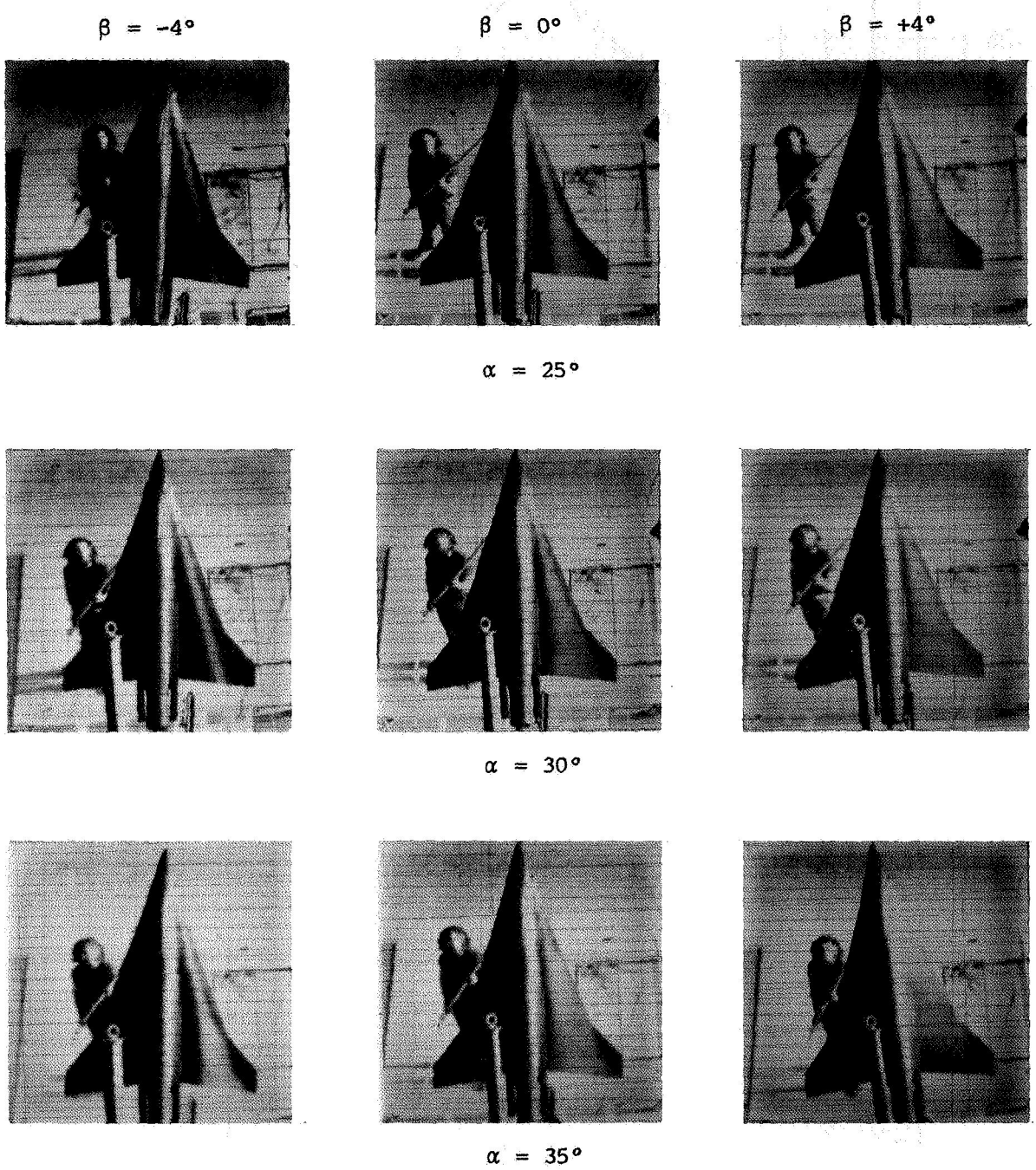

L-84-43

Figure 5.- Smoke flow visualization showing vortex breakdown on baseline configuration.

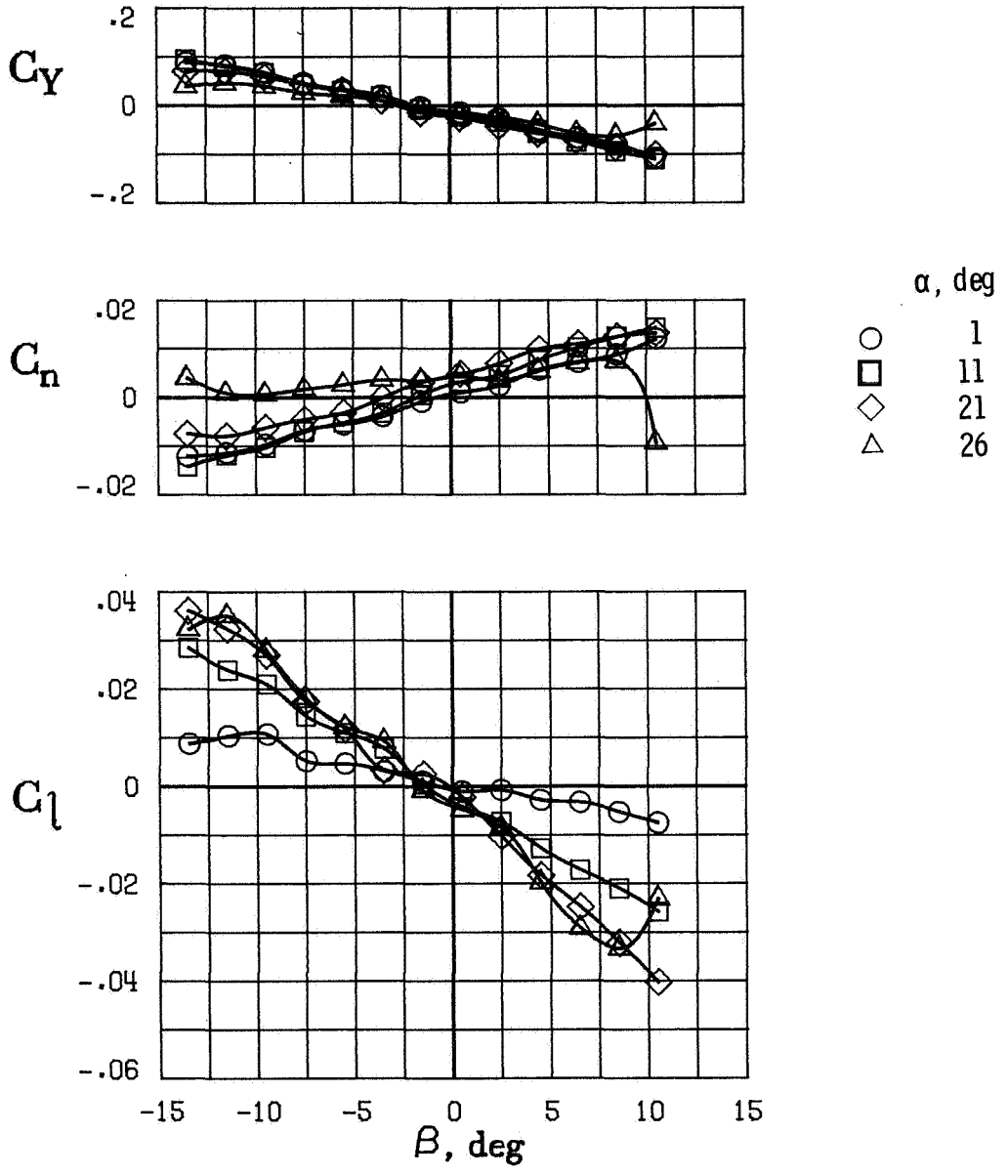

Figure 6.- Variation of static lateral-directional coefficients with sideslip angle. Baseline configuration.

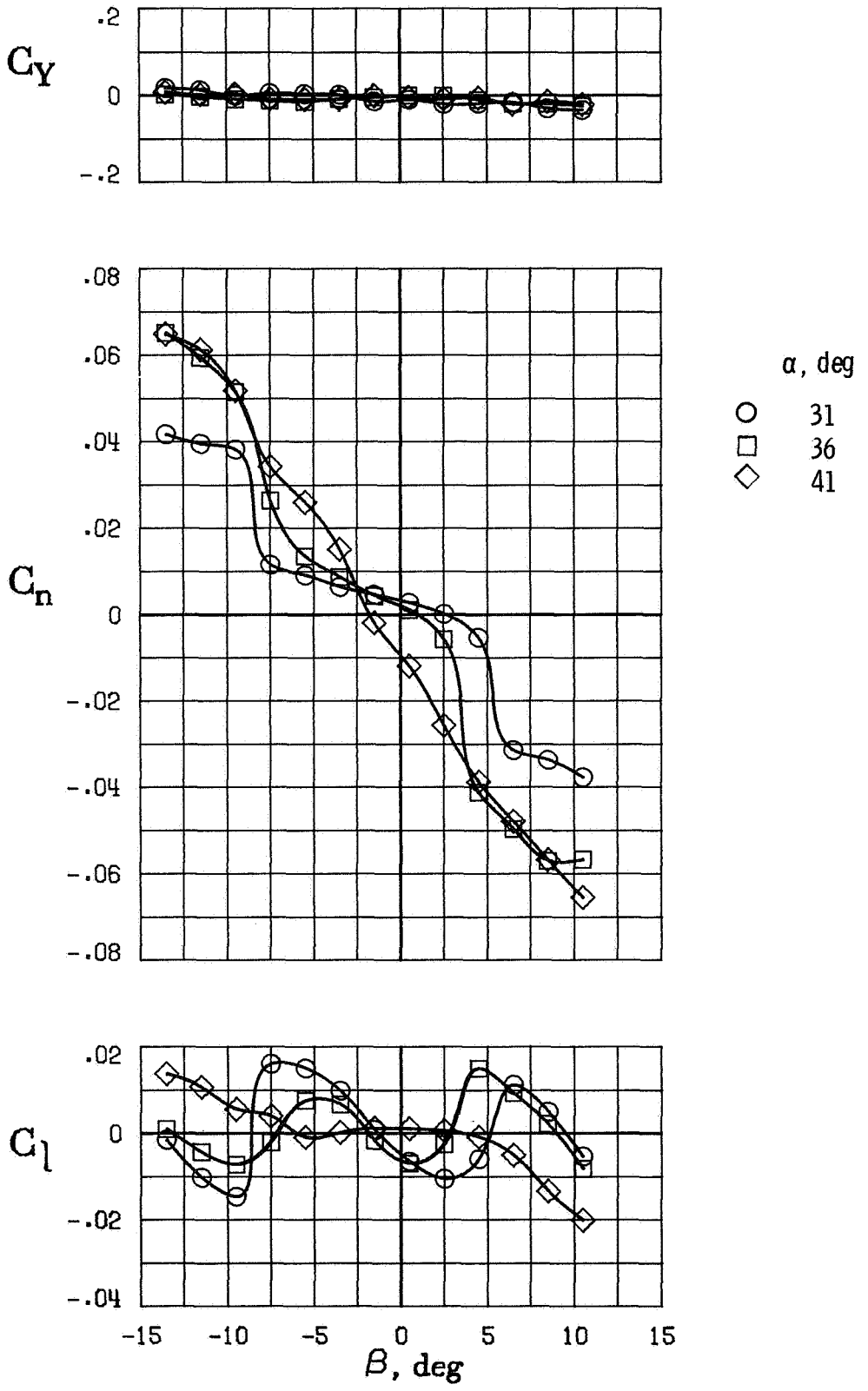

Figure 6.- Concluded.

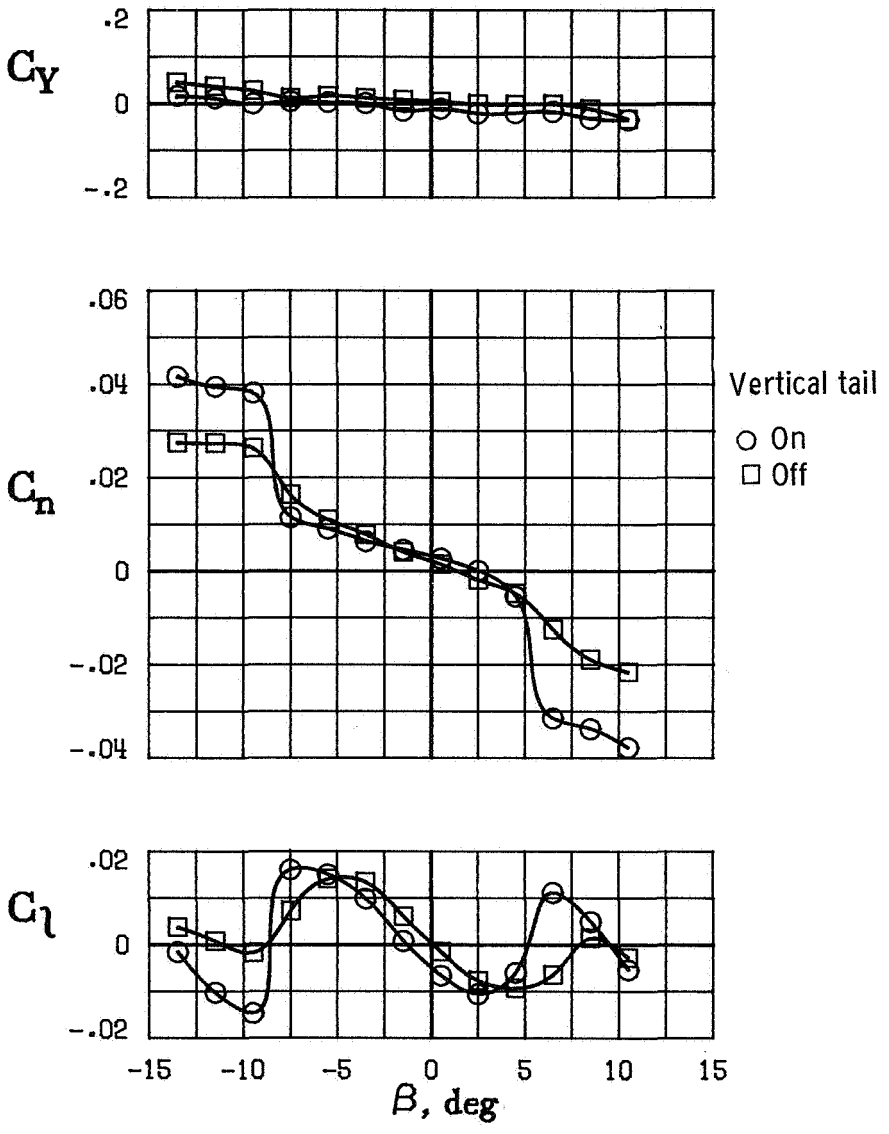

(a) $\alpha = 31°$.

Figure 7.- Variation of static lateral-directional coefficients for baseline configuration with vertical tail off and on.

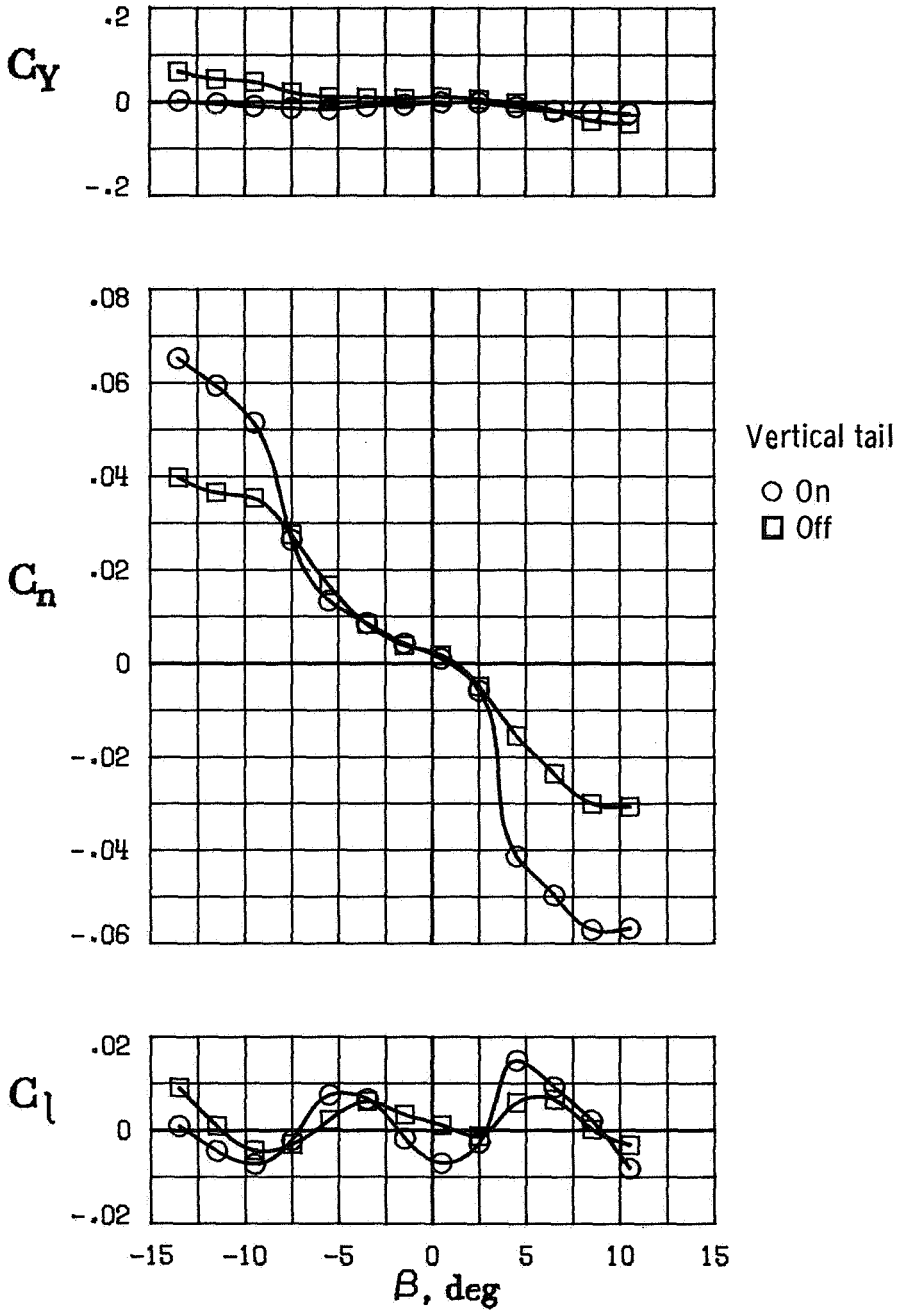

(b) $\alpha = 36°$.

Figure 7.- Continued.

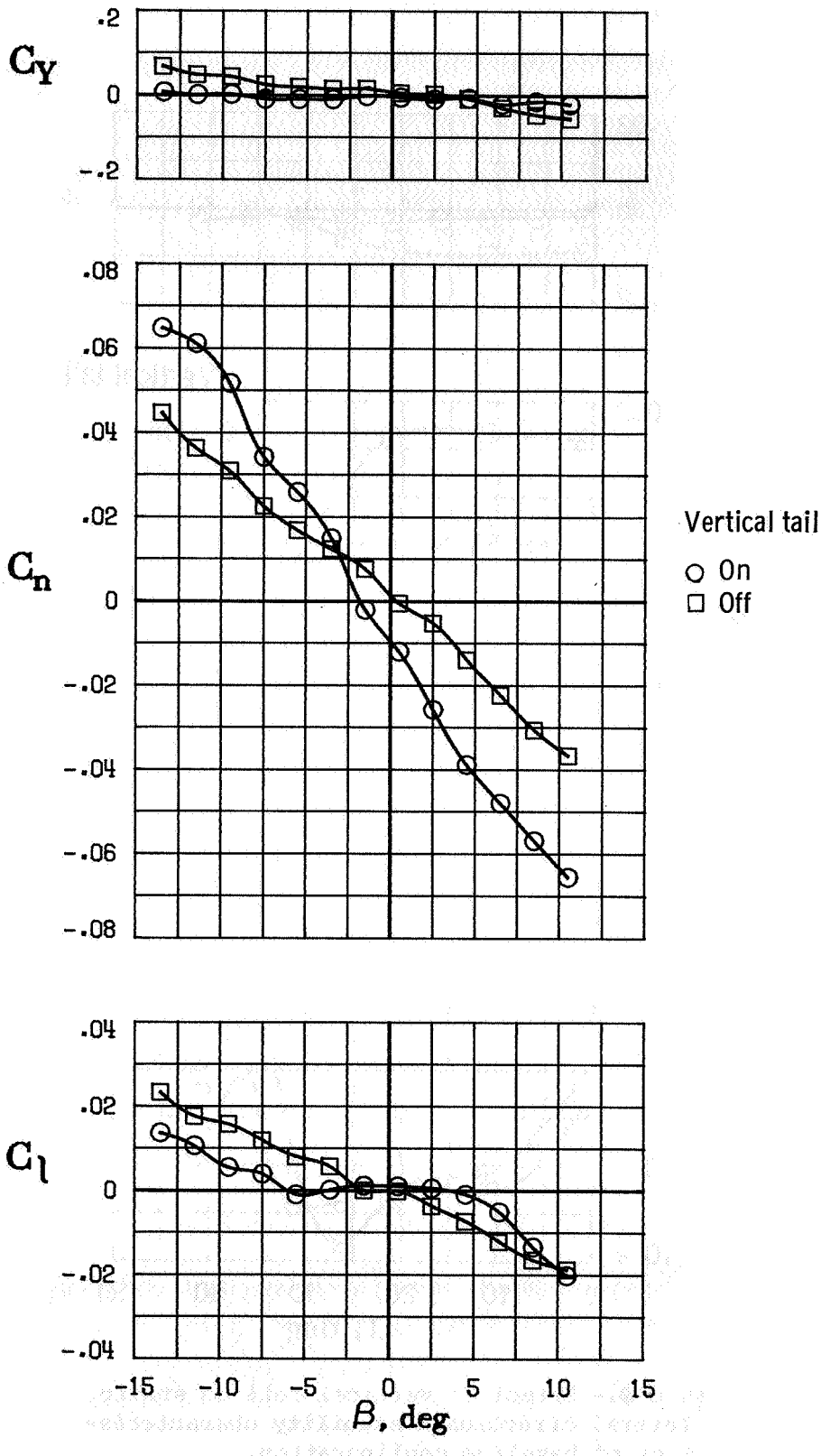

(c) $\alpha = 41°$.

Figure 7.- Concluded.

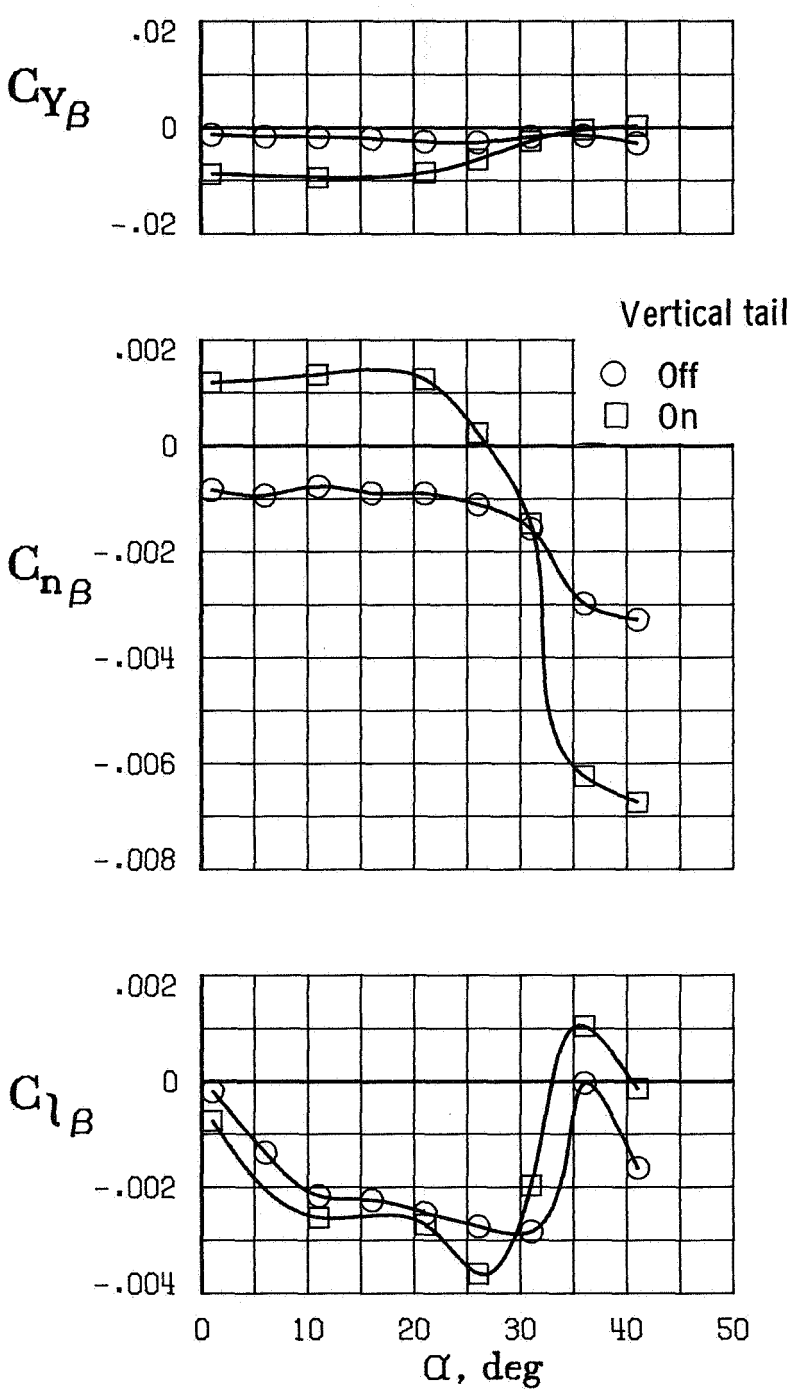

Figure 8.- Effect of vertical tail on static lateral-directional stability characteristics of baseline configuration.

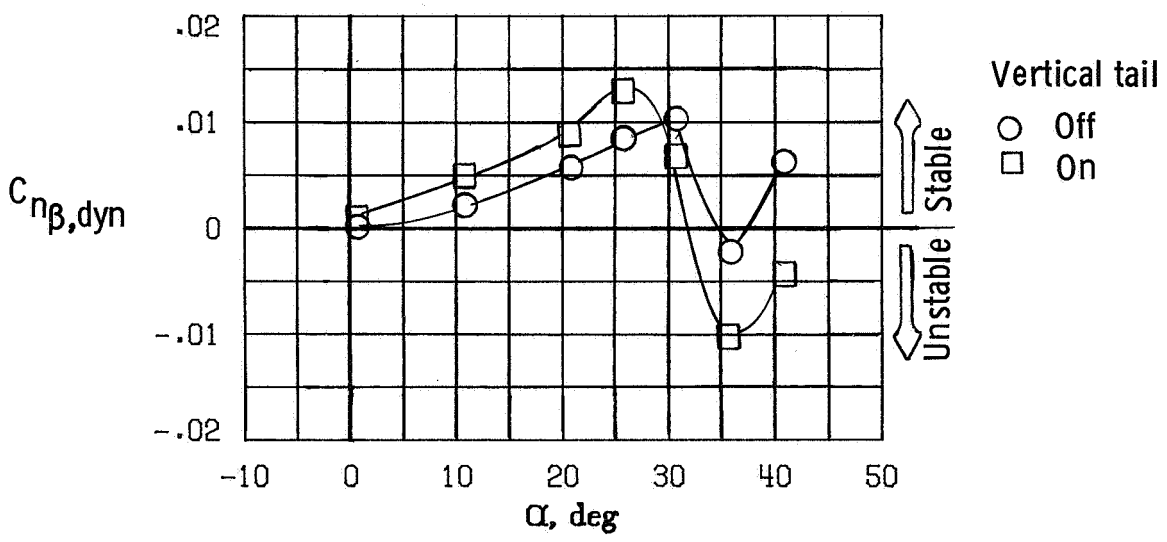

Figure 9.- Variation of $C_{n_{\beta,dyn}}$ with angle of attack. Baseline configuration.

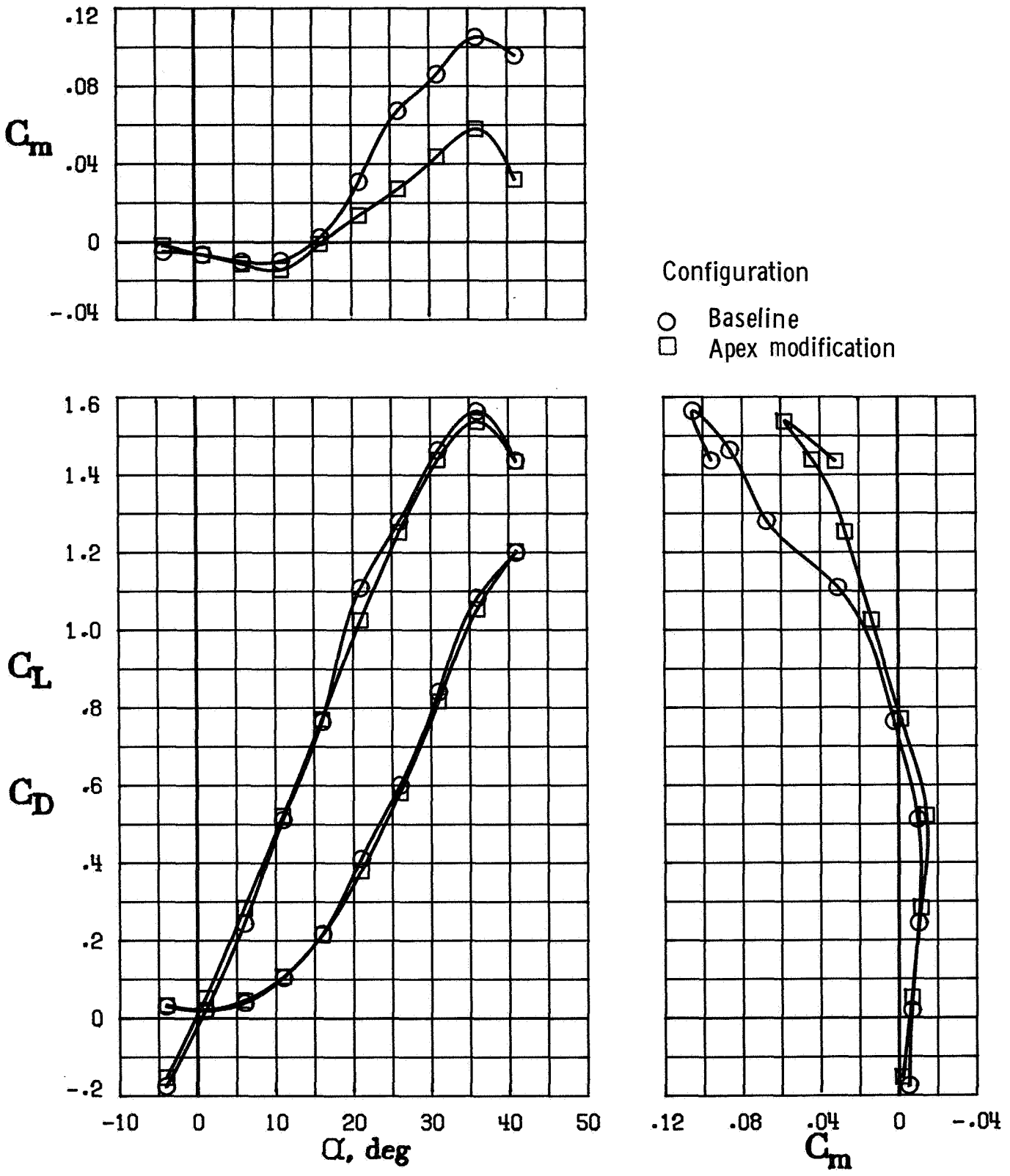

Figure 10.- Effect of apex modification on static longitudinal aerodynamic characteristics. Vertical tail off.

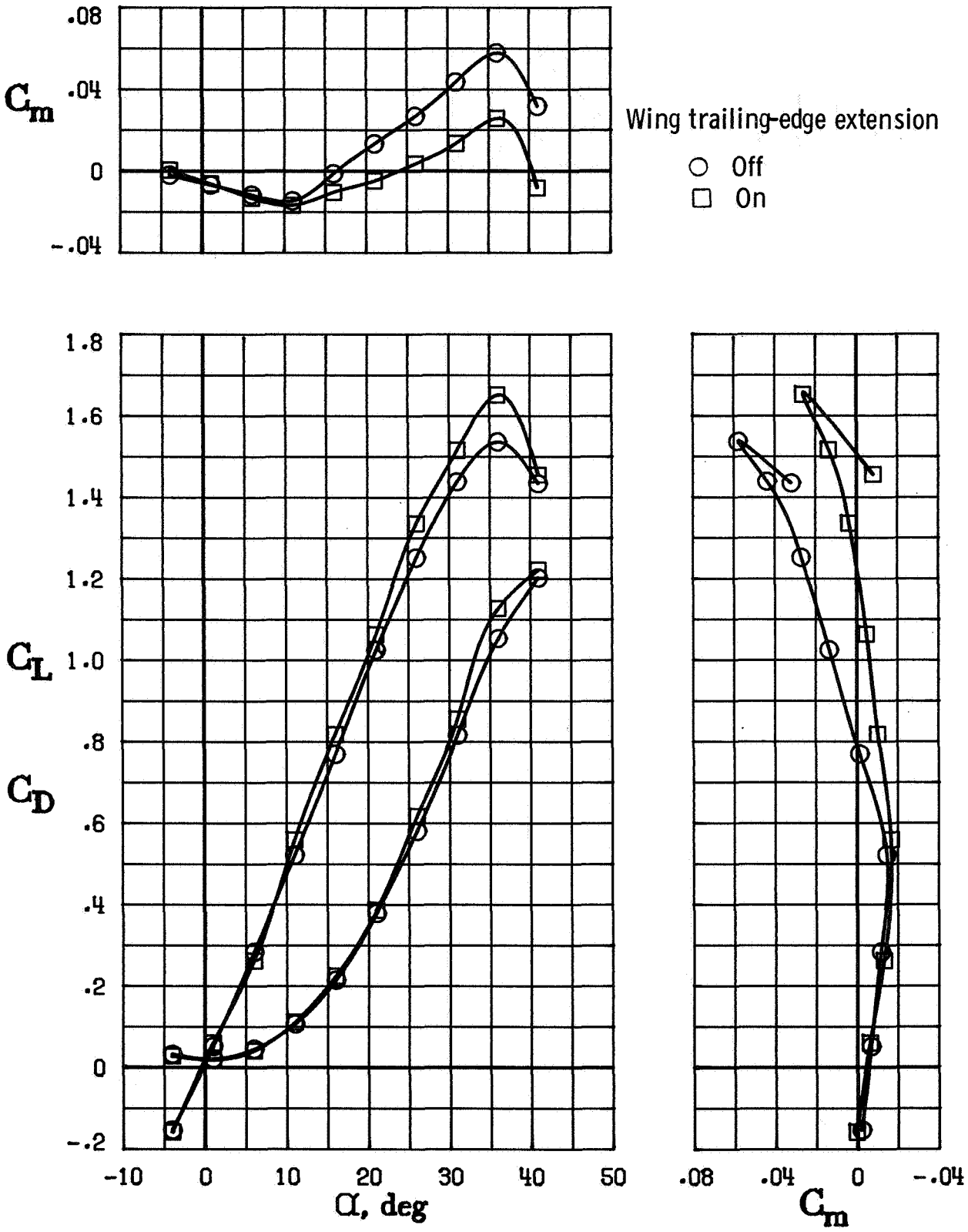

Figure 11.- Effect of wing trailing-edge extension on static longitudinal aerodynamic characteristics. Vertical tail off; apex modification on.

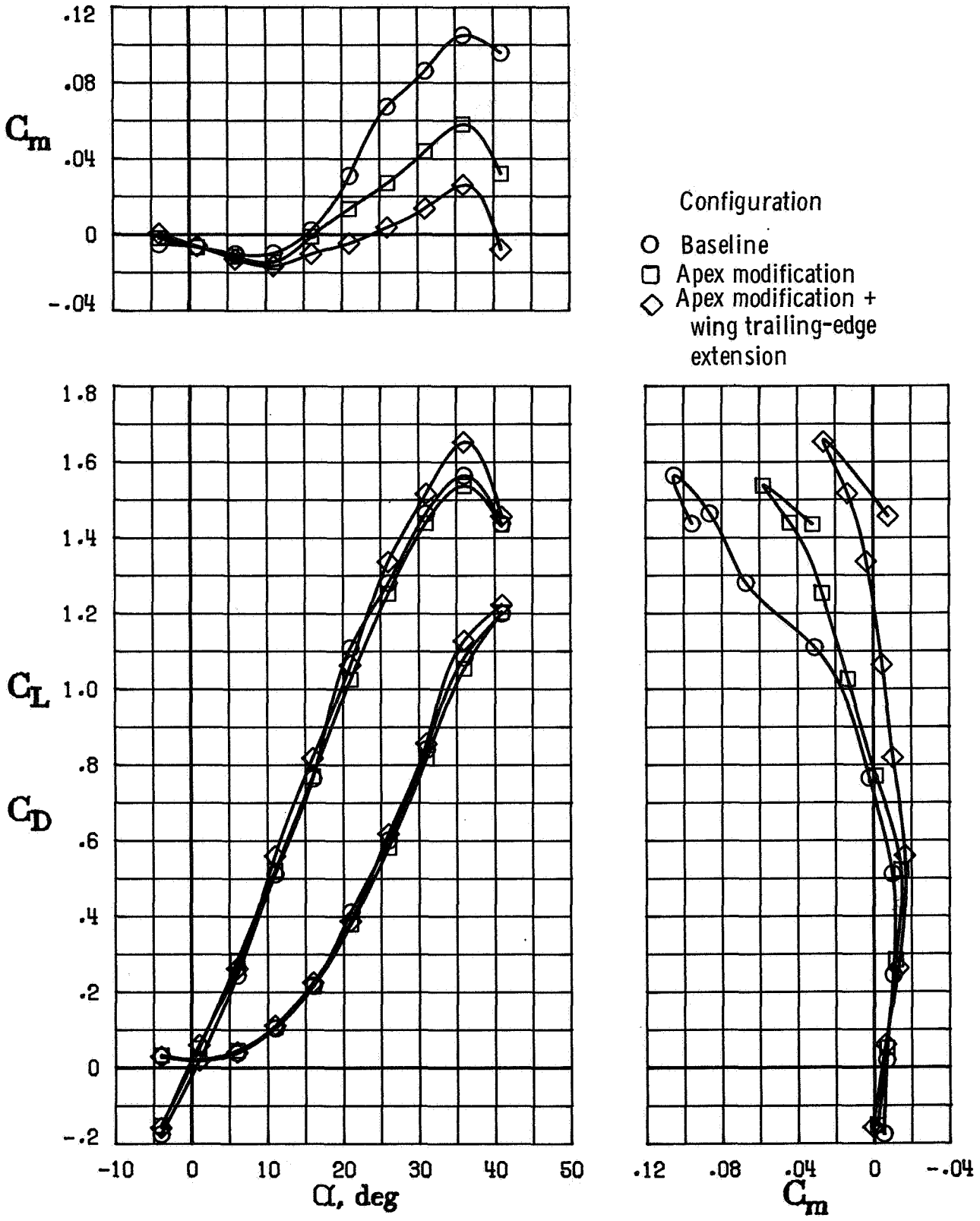

Figure 12.- Effect of apex notch and wing trailing-edge extension on static longitudinal aerodynamic characteristics.

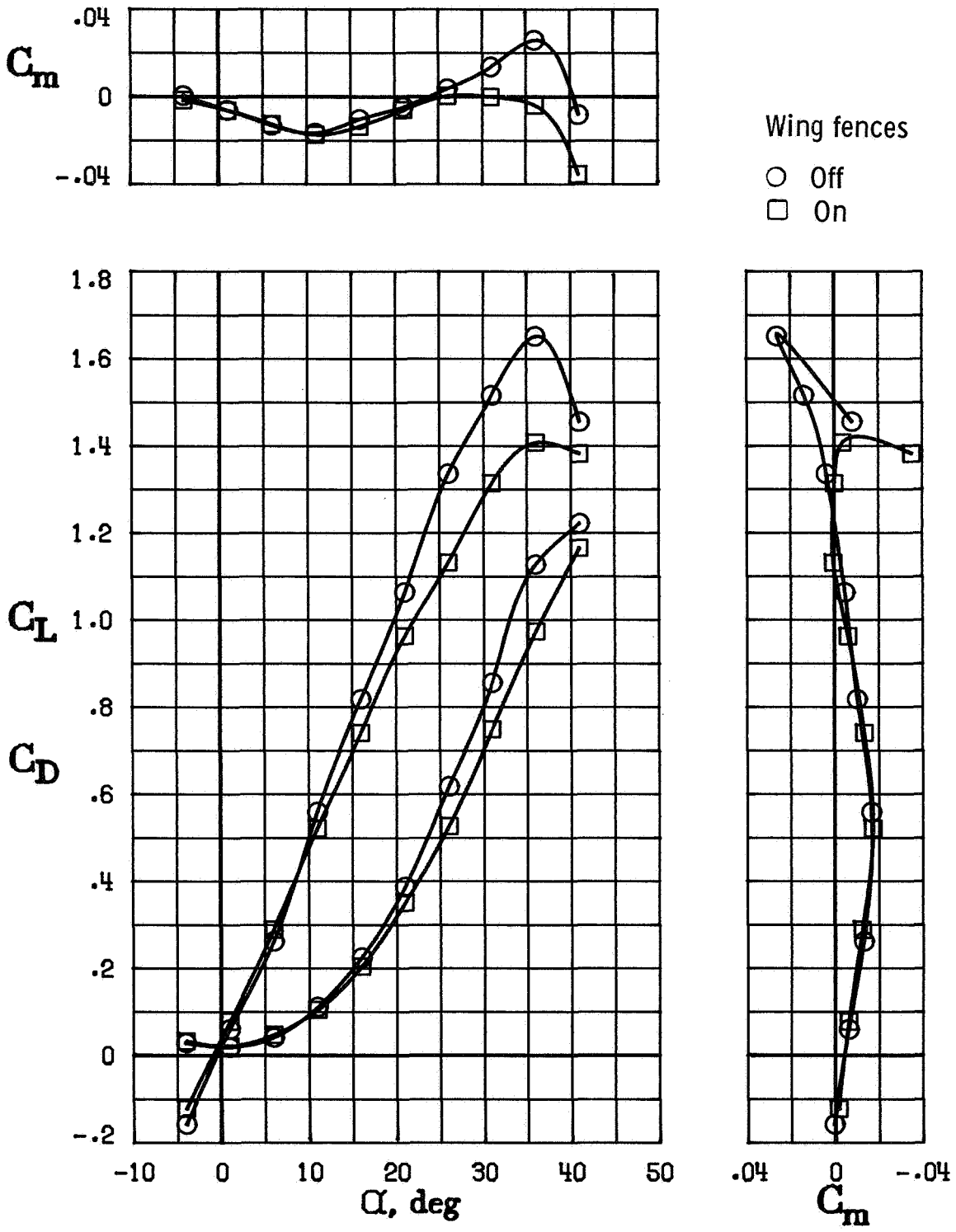

Figure 13.- Effect of wing fences on static longitudinal aerodynamic characteristics. Vertical tail off; apex modification on; wing trailing-edge extension on.

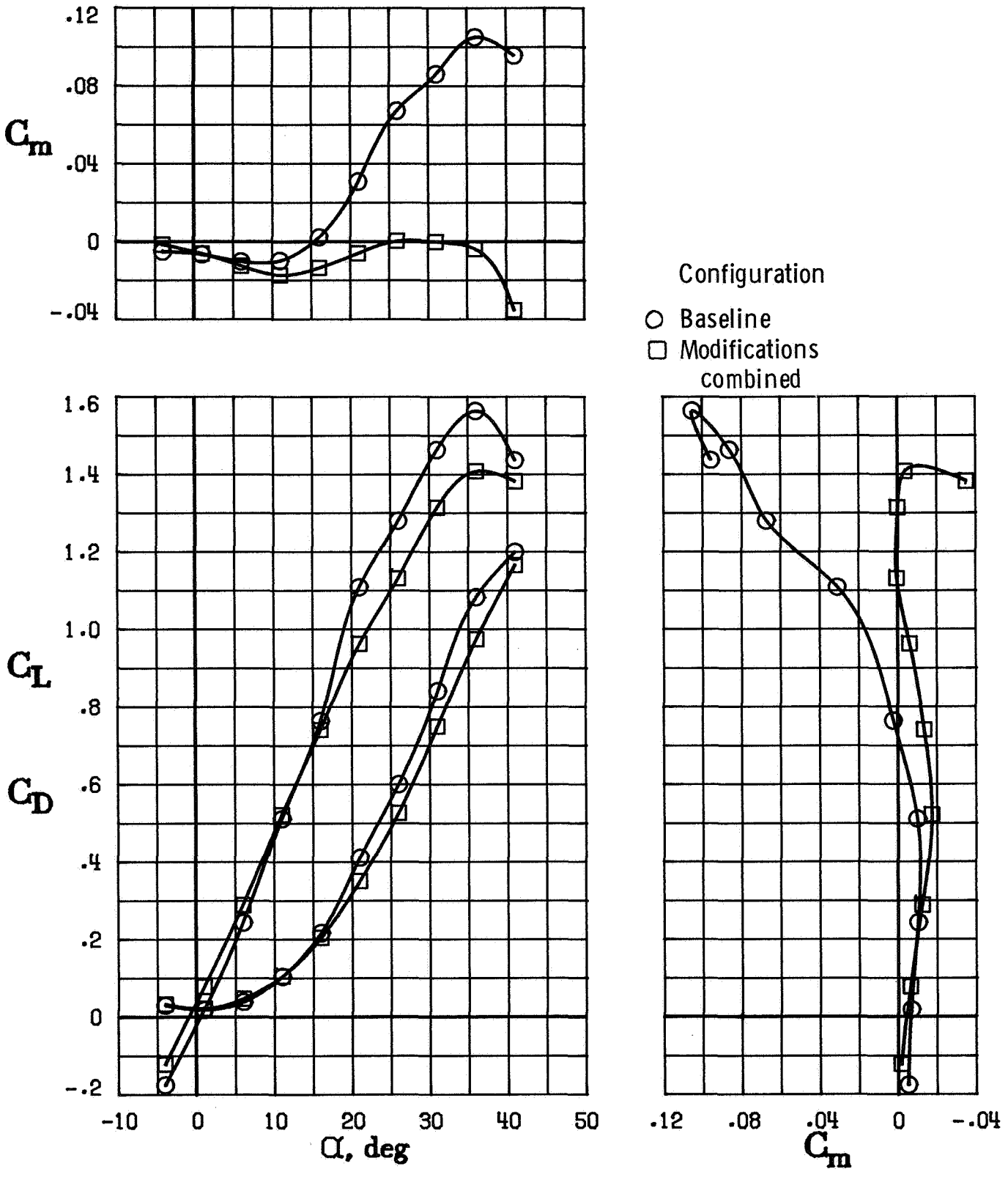

Figure 14.- Effect of combination of apex notch, wing trailing-edge extension, and fences on static longitudinal aerodynamic characteristics. Vertical tail off.

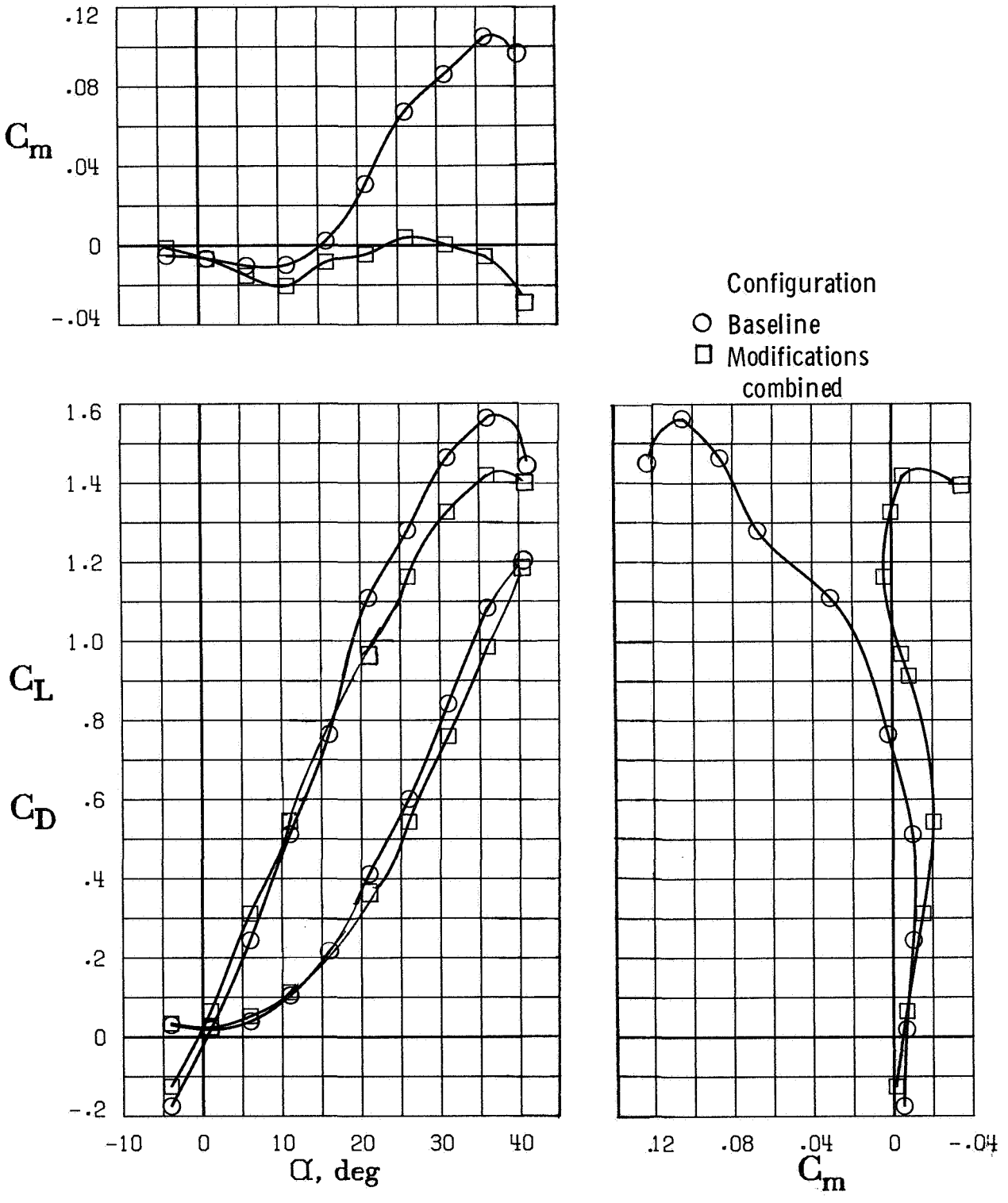

Figure 15.- Effect of combination of apex notch, wing trailing-edge extension, and fences on static longitudinal aerodynamic characteristics. Vertical tail on.

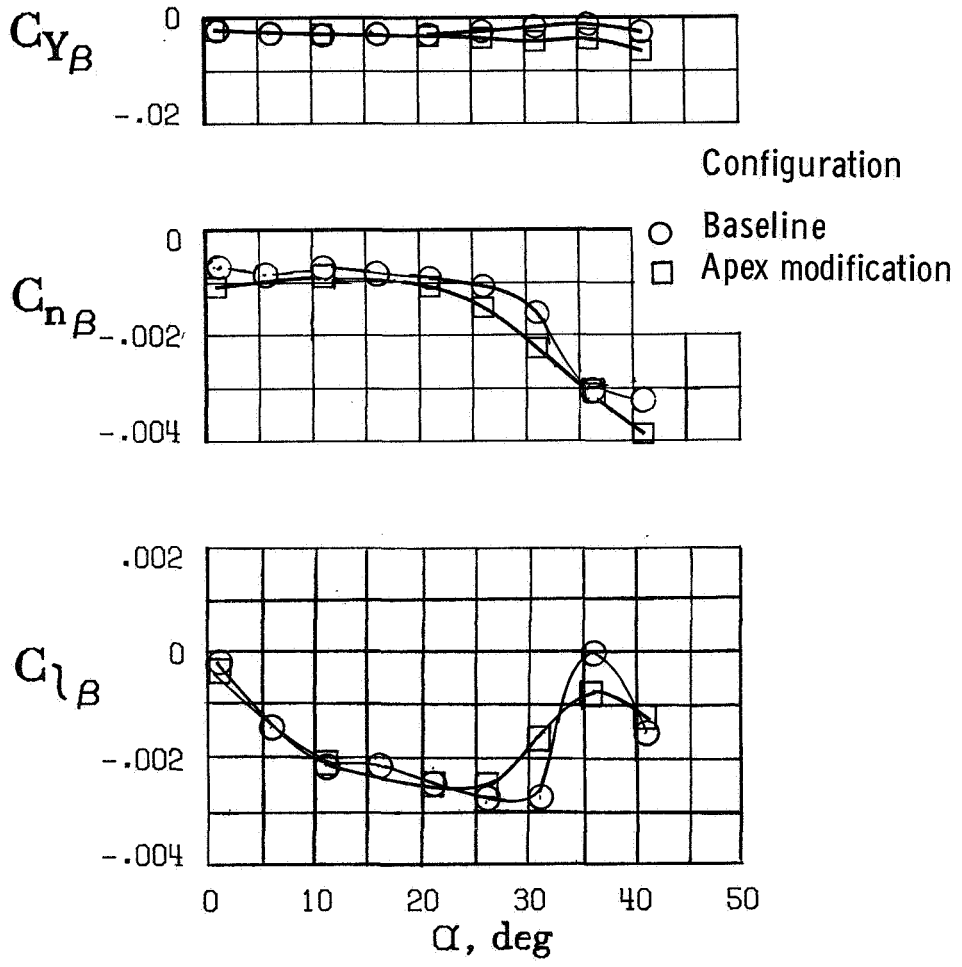

Figure 16.- Effect of apex modification on lateral-directional stability characteristics of baseline configuration.

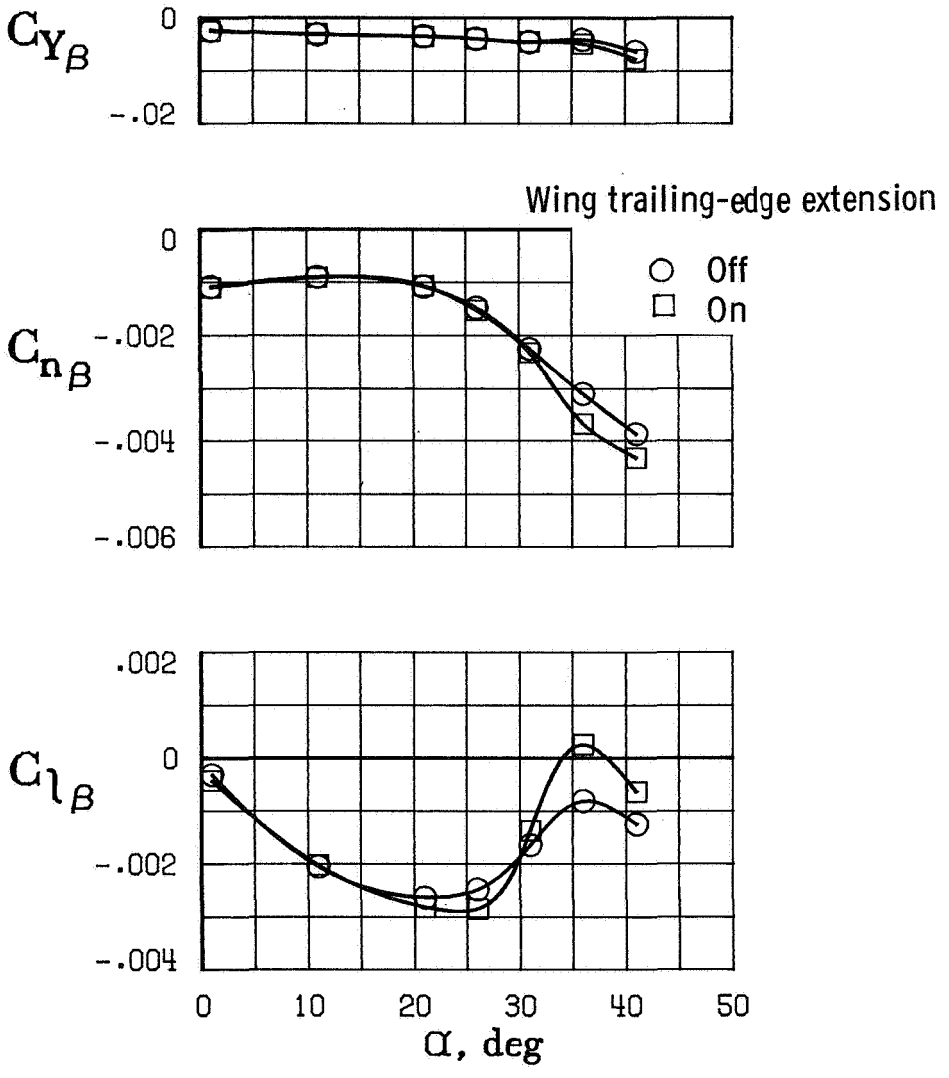

Figure 17.- Effect of wing trailing-edge extension on lateral-directional stability characteristics of baseline configuration. Apex modification on; vertical tail off.

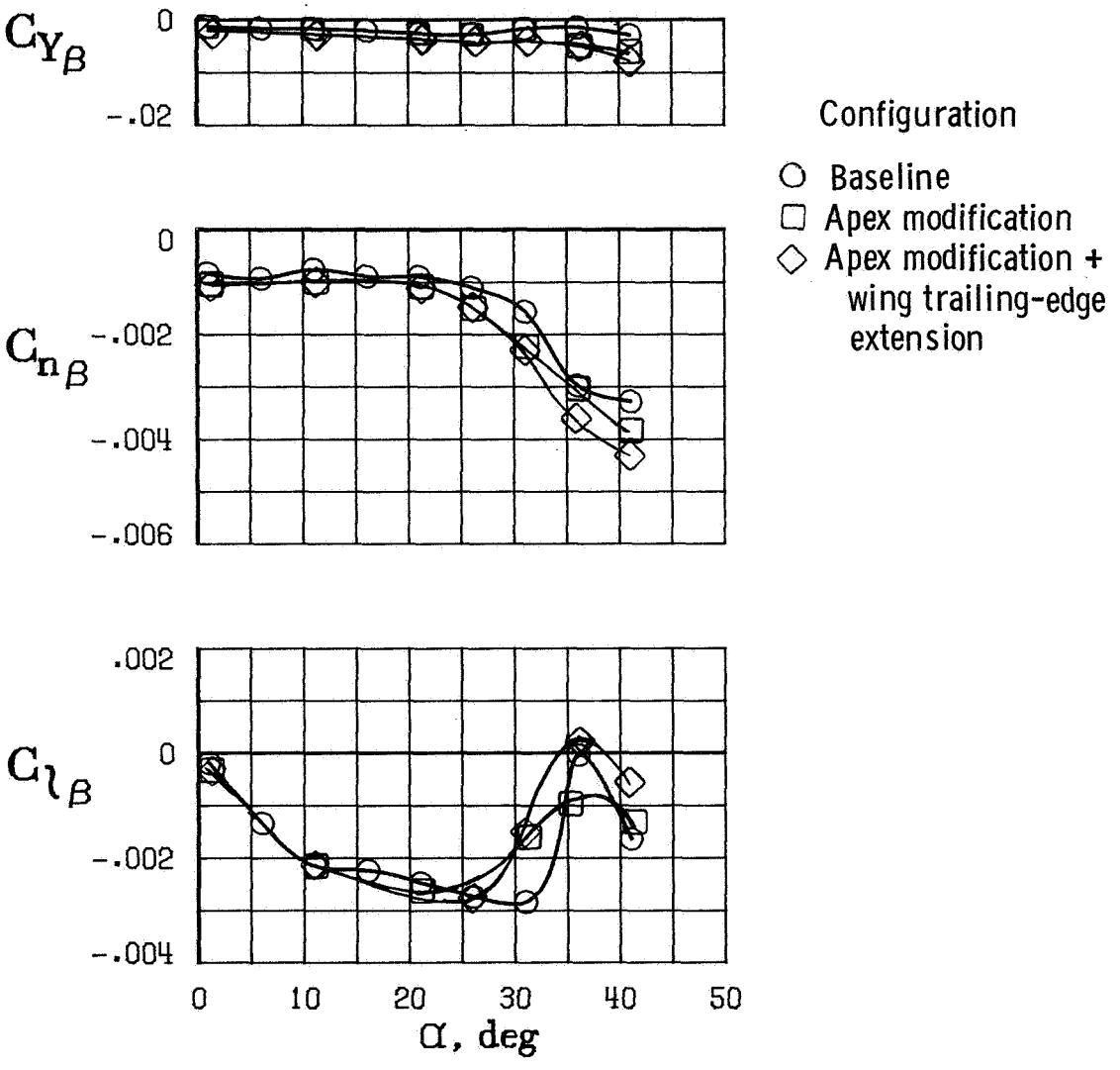

Figure 18.- Effect of combination of wing apex notch and wing trailing-edge extension on lateral-directional stability characteristics of test configuration. Vertical tail off.

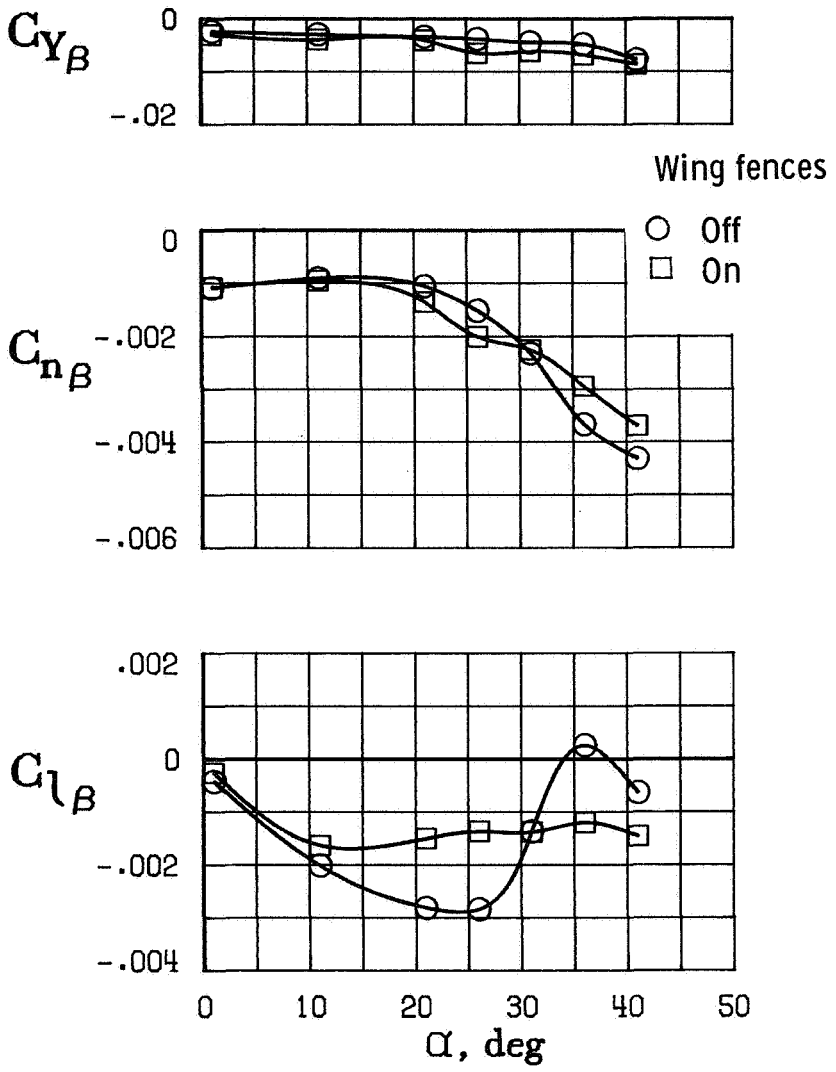

Figure 19.- Effect of wing fences on lateral-directional stability characteristics of test configuration. Vertical tail off; apex modification and wing trailing-edge extension on.

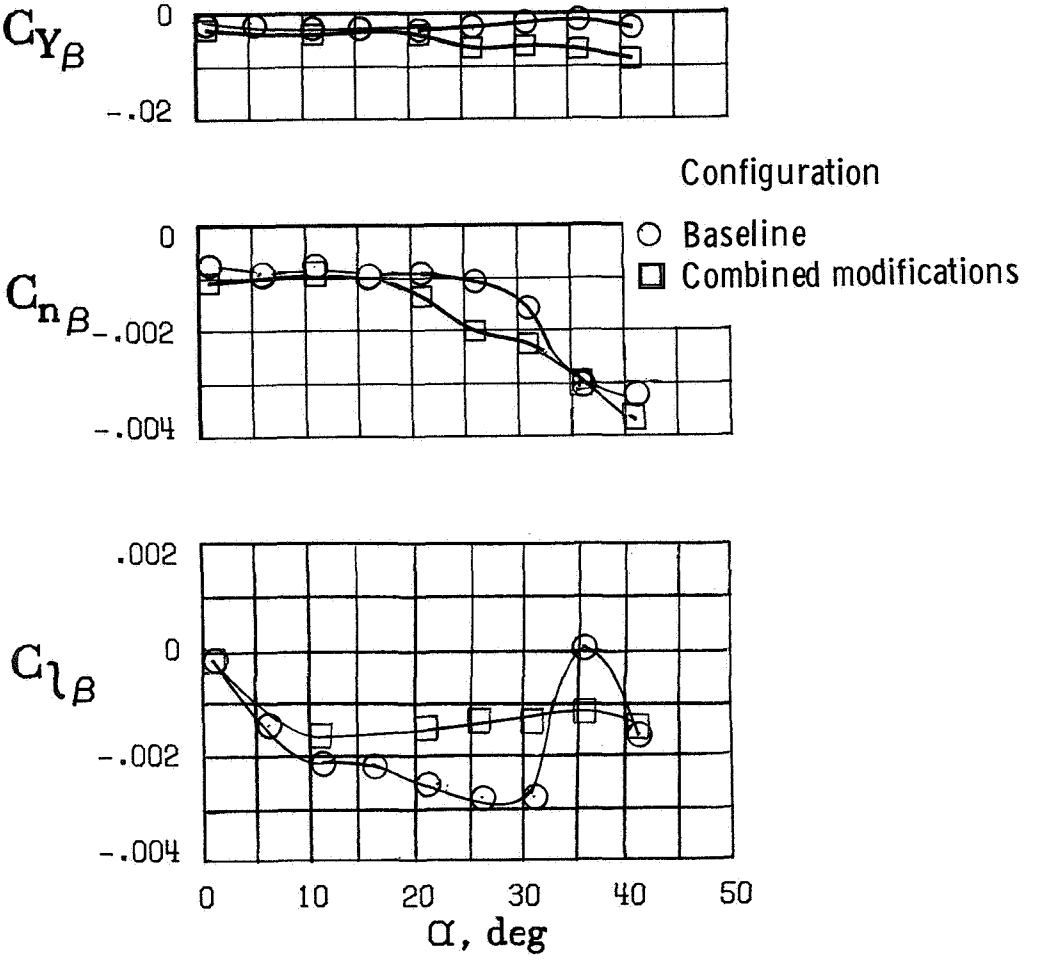

Figure 20.- Effect of combination of wing apex notch, wing trailing-edge extension, and wing fences on lateral-directional stability characteristics of baseline configuration. Vertical tail off.

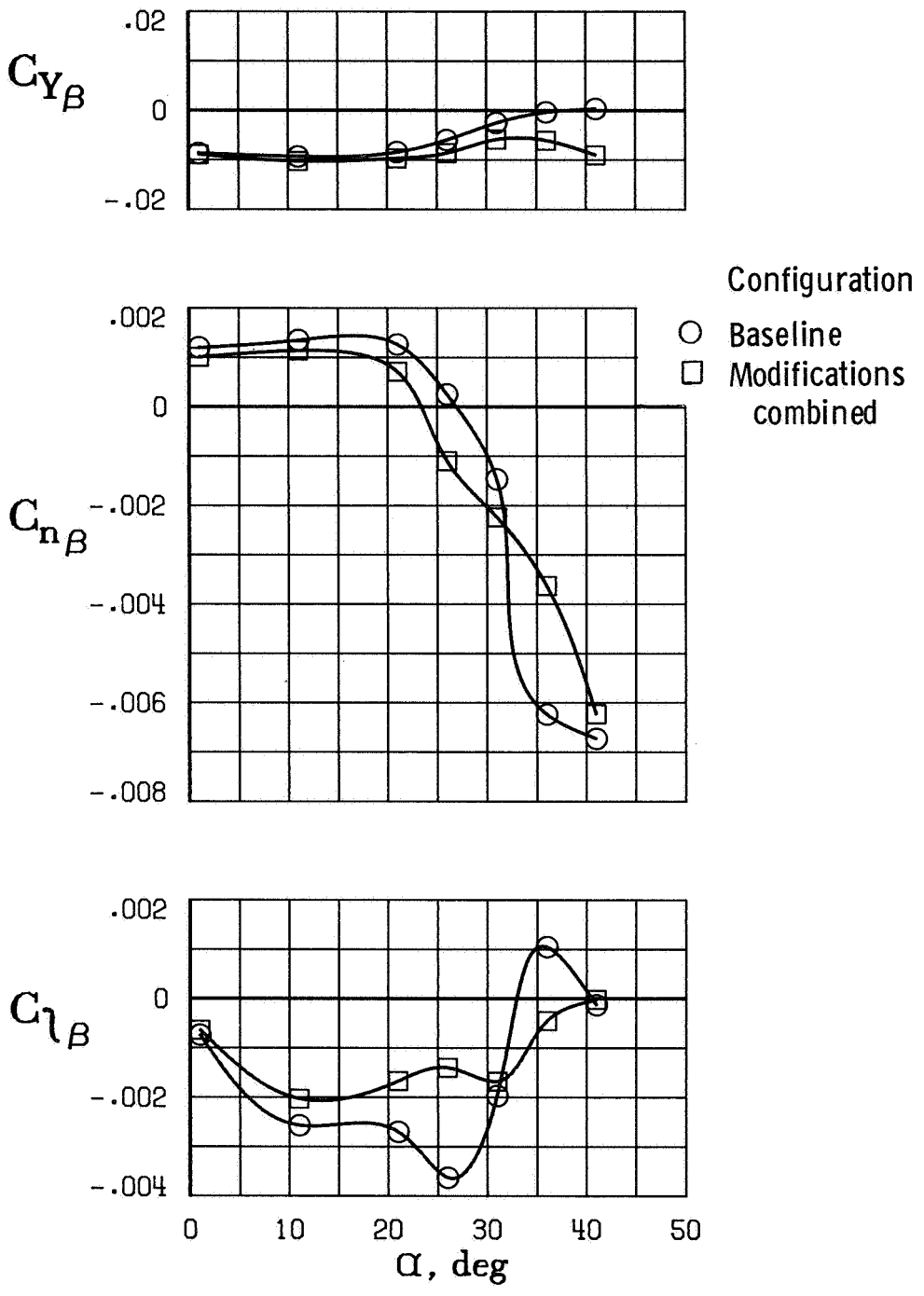

Figure 21.- Effect of combination of wing apex notch, wing trailing-edge extension, and wing fences on lateral-directional stability characteristics of baseline configuration. Vertical tail on.

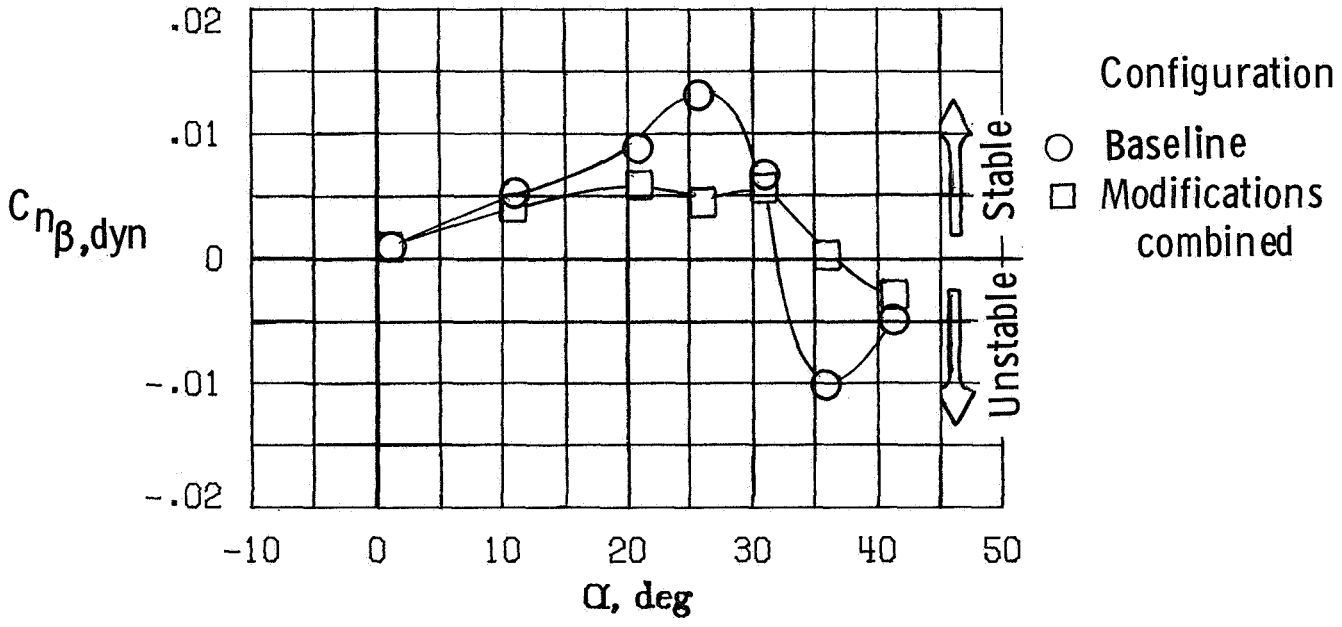

Figure 22.- Effect of combined modifications on variation of $C_{n_{\beta,dyn}}$ with angle of attack. Vertical tail on.

1. Report No.	2. Government Accession No.	3. Recipient's Catalog No.
NASA TM-85776		

4. Title and Subtitle	5. Report Date
LOW-SPEED WIND-TUNNEL STUDY OF THE HIGH-ANGLE-OF-ATTACK STABILITY AND CONTROL CHARACTERISTICS OF A CRANKED-ARROW-WING FIGHTER CONFIGURATION	May 1984
	6. Performing Organization Code 505-43-13-01
7. Author(s) Sue B. Grafton	8. Performing Organization Report No. L-15762
	10. Work Unit No.
9. Performing Organization Name and Address NASA Langley Research Center Hampton, VA 23665	11. Contract or Grant No.
	13. Type of Report and Period Covered Technical Memorandum
12. Sponsoring Agency Name and Address National Aeronautics and Space Administration Washington, DC 20546	14. Sponsoring Agency Code

15. Supplementary Notes

16. Abstract

The low-speed, high-angle-of-attack stability and control characteristics of a fighter configuration incorporating a cranked arrow wing were investigated in the Langley 30- by 60-Foot Tunnel. The study was conducted as part of a NASA/General Dynamics cooperative research program to investigate the application of advanced wing designs to combat aircraft. Tests were conducted on a baseline configuration and on several modified configurations. The results of the investigation showed that the baseline configuration exhibited a high level of maximum lift but displayed undesirable longitudinal and lateral-directional stability characteristics at high angles of attack. Various wing modifications were made which improved the longitudinal and lateral-directional stability characteristics of the configuration at high angles of attack. However, most of the modifications were detrimental to maximum lift.

17. Key Words (Suggested by Author(s))
Arrow wings
Fighter
Stability
Longitudinal
Lateral directional
Static

18. Distribution Statement
Unclassified - Unlimited

Subject Category 08

19. Security Classif. (of this report)	20. Security Classif. (of this page)	21. No. of Pages	22. Price
Unclassified	Unclassified	37	A03

For sale by the National Technical Information Service, Springfield, Virginia 22161

NASA-Langley, 1984